

---

Masters Theses

Student Theses and Dissertations

---

Spring 2002

## Glass transition behavior of thin poly(methyl methacrylate) films on silica

Moses T. Kabomo

Follow this and additional works at: [https://scholarsmine.mst.edu/masters\\_theses](https://scholarsmine.mst.edu/masters_theses)

 Part of the [Chemistry Commons](#)

Department:

---

### Recommended Citation

Kabomo, Moses T., "Glass transition behavior of thin poly(methyl methacrylate) films on silica" (2002). *Masters Theses*. 2151.  
[https://scholarsmine.mst.edu/masters\\_theses/2151](https://scholarsmine.mst.edu/masters_theses/2151)

This thesis is brought to you by Scholars' Mine, a service of the Missouri S&T Library and Learning Resources. This work is protected by U. S. Copyright Law. Unauthorized use including reproduction for redistribution requires the permission of the copyright holder. For more information, please contact [scholarsmine@mst.edu](mailto:scholarsmine@mst.edu).

GLASS TRANSITION BEHAVIOR OF THIN POLY(METHYL METHACRYLATE)  
FILMS ON SILICA

by

MOSES TLHABOLOGO KABOMO

A THESIS

Presented to the Faculty of the Graduate School of the

UNIVERSITY OF MISSOURI-ROLLA

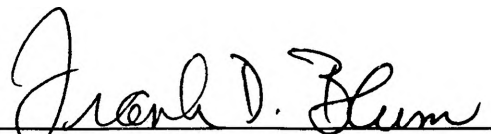
In Partial Fulfillment of the Requirements for the Degree

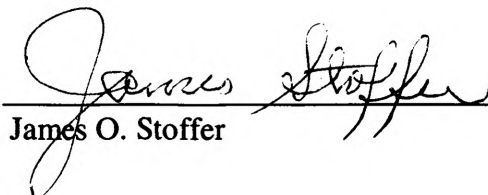
MASTER OF SCIENCE IN CHEMISTRY

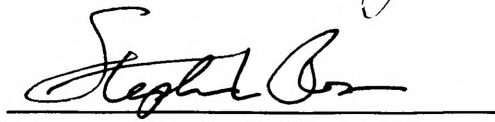
2002

T8066  
81 pages

Approved by

  
Frank D. Blum, Advisor

  
James O. Stoffer

  
Stephen L. Rosen

## PUBLICATION THESIS OPTION

This thesis has been prepared in the style utilized by the ACS journal *Macromolecules*. Pages 30-57 will be submitted for publication in that journal or one of ACS journals. Appendices A and B have been added for purposes normal to thesis writing.

## ABSTRACT

Modulated Differential Scanning Calorimetry (MDSC) was used to study the glass transition behavior of poly(methyl methacrylate) (PMMA) adsorbed onto silica substrates from toluene. Untreated fumed amorphous silica and silica treated with hexamethyldisilazane were used for the adsorption to probe the effect of polymer-substrate interactions. To test the effect of molecular weight on the  $T_g$  of adsorbed polymers, low polydispersity PMMA samples of varying molecular weights were used. The results revealed a broadening of the glass transition towards high temperatures. The observed increase in the glass transition breadth varied with adsorbed amount and the type of silica used for the adsorption. Larger increases in the glass transition temperature and breadth, as high as 60 °C, were observed for PMMA films on untreated silica. The larger increase in  $T_g$  was attributed to restricted segmental motions due to H-bonding between PMMA carbonyls and the surface hydroxyls.

The MDSC results were verified by Fourier Transform Infrared (FTIR) spectroscopy which showed a decrease in the bound fraction with increasing adsorbed amount for all the molecular weights studied.

## **ACKNOWLEDGMENTS**

I would like to thank my advisor Dr Frank D. Blum for the guidance and assistance he afforded me during my study. I would also like to thank my Advisory Committee members Dr James O. Stoffer and Dr Stephen L. Rosen.

## TABLE OF CONTENTS

	Page
PUBLICATION THESIS OPTION .....	iii
ABSTRACT.....	iv
ACKNOWLEDGMENTS .....	v
LIST OF ILLUSTRATIONS .....	viii
LIST OF TABLES .....	xi
1. INTRODUCTION .....	1
2. BACKGROUND .....	3
2.1. GLASS TRANSITION OF POLYMERS.....	3
2.1.1. The Free Volume Theory .....	3
2.1.2. The Thermodynamic Theory.....	6
2.1.3. The Kinetic Theory .....	7
2.1.4. Factors that Influence $T_g$ .....	9
2.1.4.1 Molecular Weight .....	10
2.1.4.2 Copolymerization .....	11
2.1.4.3 Cross-linking .....	11
2.1.4.4 Tacticity.....	12
2.1.4.5 Plasticizers.....	13
2.2. ADSORPTION OF POLYMERS ON SURFACES.....	14
2.2.1. Polymer Chain Conformations .....	15
2.2.2. Driving Force for Adsorption.....	17

2.2.3. Formation of an Adsorbed Layer.....	18
2.2.4. Conformation of the Adsorbed Layer .....	20
2.3. MODULATED DIFFERENTIAL SCANNING CALORIMETRY (MDSC)..	21
2.4. REFERENCE .....	27
3. MDSC AND FTIR STUDY OF THE GLASS TRANSITION OF POLY(METHYL METHACRYLATE) ADSORBED ON SILICA.....	30
3.1. Abstract .....	30
3.2. Introduction .....	30
3.3. Experimental.....	32
3.4. Results and Discussion.....	34
3.5. Conclusion.....	52
3.6. Reference.....	56
<b>APPENDICES</b>	
A. DETERMINATION OF ADSORBED AMOUNT BY THERMOGRAVIMETRIC ANALYSIS .....	58
B. INFRARED SPECTROSCOPY OF PMMA THIN FILMS ON SILICA.....	65
VITA .....	70

## LIST OF ILLUSTRATIONS

Figure	Page
2.1. Variation of (a) specific volume, and (b) isothermal expansion coefficient, $\alpha$ , and compressibility factor, $\beta$ , with temperature.....	5
2.2. Effect of solvent on polymer chain dimensions.....	17
2.3. Spreading effects on adsorbed layer thickness.....	20
2.4. The loop-tail-train model of an adsorbed polymer.....	20
2.5. MDSC heating profile with an underlying heating rate of 2.5 °C/minute, a modulation period of 60 seconds, and a modulation period of $\pm 1$ °C.....	24
2.6. MDSC data for a PMMA sample showing the complex raw data and the deconvoluted heat flow curve.....	25
2.7. MDSC data for a PMMA sample showing the total heat flow and its two components, the reversing heat flow and the non-reversing heat flow.....	26
3.1. MDSC curves (derivative of the reversing heat flow) of bulk PMMA samples. The $T_g$ 's are taken as the peak maxima.....	35
3.2. MDSC curves of bulk P19MMA and P19MMA adsorbed on M5 from 5 mg/mL (solid) and 10 mg/mL (dash) solutions. ....	36
3.3. MDSC curves of bulk P49MMA and P49MMA adsorbed on M5 from 5 mg/mL (solid) and 10 mg/mL (dash) solutions. ....	37
3.4. MDSC curves of bulk P216MMA and P216MMA adsorbed on M5 from 5 mg/mL (solid) and 10 mg/mL (dash) solutions.....	38
3.5. FTIR spectra of bulk PMMA and P19MMA adsorbed on M5 in the region of the carbonyl absorption.....	45



3.6. FTIR spectra of bulk PMMA and P49MMA adsorbed on M5 in the region of the carbonyl absorption.....	46
3.7. FTIR spectra of bulk PMMA and P216MMA adsorbed on M5 in the region of the carbonyl absorption. ....	47
3.8. FTIR spectra of bulk PMMA and P587MMA adsorbed on M5 in the region of the carbonyl absorption. ....	48
3.9. MDSC curves of PMMA adsorbed on TS530 from 10 mg/mL solutions. ....	53
3.10. FTIR spectra of bulk PMMA and PMMA adsorbed on TS530 in the region of the carbonyl absorption. ....	54
A.1. Determination of the adsorbed amount by TGA. The sample was ramped from ambient temperature to 600 °C at a heating rate of 10 °C/min. ....	60
A.2. TGA curves for the determination of adsorbed amount of P19MMA-0.8 and P19MMA-1.8. The samples were ramped from ambient temperature to 600 °C at 10 °C/min under nitrogen purge .....	61
A.3. TGA curves for the determination of adsorbed amount of P49MMA-0.8 and P49MMA-1.8. The samples were ramped from ambient temperature to 600 °C at 10 °C/min under nitrogen purge .....	62
A.4. TGA curves for the determination of adsorbed amount of P216MMA-0.8 and P216MMA-1.8. The samples were ramped from ambient temperature to 600 °C at 10 °C/min under nitrogen purge.....	63
A.5. TGA curves for the determination of adsorbed amount of P19MMA-0.8 and P19MMA-1.8. The samples were ramped from ambient temperature to 600 °C at 10 °C/min under nitrogen purge .....	64
B.1. FTIR spectrum of bulk PMMA acquired on a film cast for m toluene. 1024 scans were performed to get good signal-to-noise ratio.....	67
B.2. FTIR spectrum of silica-adsorbed PMMA acquired on a film cast for m toluene. 1024 scans were performed to get good signal-to-noise ratio.....	68

B.3. FTIR curve-fitted carbonyl band of PMMA adsorbed on untreated silica (M5) from 0.5% toluene solution. ....	69
--	----

## LIST OF TABLES

Table	Page
3.1. Polymer Samples of Poly(methyl methacrylate).....	39
3.2. Thermal Characterization of the PMMA thin films adsorbed from 0.5% toluene solutions. ....	41
3.3. Thermal Characterization of the PMMA thin films adsorbed from 1% toluene solutions ....	43
3.4. Bound Fractions for the PMMA Adsorbed Samples.....	49
3.5. Thermal Characterization of the PMMA thin films adsorbed from 0.5% toluene solutions onto TS530 (treated silica). ....	55

## 1. INTRODUCTION

The adsorption of polymers on solid substrates determines the structure of the boundary layer, the type of packing of the macromolecules in the boundary layer, and hence the molecular mobility of the chains, and their relaxation and other properties.<sup>1</sup> After extensive studies on filled polymer systems, Lipatov and Seergeva concluded that the properties of polymer films are determined by the fraction of polymer at the polymer-substrate interface. The properties of the polymer films deviate from bulk behavior as the film gets thinner and thinner. Frank *et al.* described as “ultrathin” a polymer film of thickness less than 1000 Å and as “thin” for thicknesses between 1000 and 10,000 Å (1 μm).<sup>2</sup> Recent studies now show that the properties of ultrathin and thin polymer films differ substantially from bulk properties.<sup>3</sup> The use of polymer thin films is found in the microelectronics industry, as alignment layers in liquid crystal displays, as lubricants in magnetic information storage devices and other numerous technologies.<sup>2</sup> With the current trend in device miniaturization, the study of the interfacial properties of polymer thin films is of paramount importance in understanding the overall behavior.

The dynamics of thin polymers has been the most widely studied property. Several experimental techniques have been employed, and these can be roughly divided into two categories; (i) those that directly probe the dynamics of polymers, and (ii) those that estimate polymer dynamics by inference from the glass transition temperature,  $T_g$ . The first group include nuclear magnetic resonance (NMR) spectroscopy,<sup>4-6</sup> dielectric relaxation spectroscopy,<sup>7,8</sup> and fluorescence recovery after photo-bleaching (FRAP).<sup>9,10</sup> The second category consist of techniques such as ellipsometry,<sup>11,12</sup> x-ray reflectivity,<sup>13</sup> and thermal analysis.<sup>14-17</sup> In general the results of these studies suggest that the mobility

of polymers in thin films can either be enhanced or depressed depending on the interaction of the polymer and the substrate. There is still, however, considerable uncertainty in the theoretical explanations for these observations.<sup>2</sup>

This work reports the use of modulated differential scanning calorimetry (MDSC) to study the glass transition behavior of poly(methyl methacrylate) ultrathin films adsorbed on silica substrates. The use of Fourier Transformation infrared (FTIR) spectroscopy to correlate the observed changes in the glass transition with the conformations of polymer chains on the silica surface is also reported. Chapter 2 focuses on the theoretical concepts of the glass transition phenomenon, the adsorption of polymers on surfaces, and MDSC. A report of my work on the glass transition behavior of PMMA thin films is given in Chapter 3.

## 2. BACKGROUND

### 2.1. GLASS TRANSITION OF POLYMERS

The glass transition temperature, perhaps the most important property of polymers, is thought to be both a kinetic and a thermodynamic phenomenon. The simplest definition of the glass transition temperature is that it is the temperature at which viscoelastic materials change from a glassy state to a viscous state as the temperature is increased. In terms of molecular motions, the glass transition temperature is defined as the temperature at which the frequency of molecular motions approaches the reciprocal of the time scale of the experiment. Several theories have been proposed to explain the glass transition phenomenon of which the free volume theory, the thermodynamic, and the kinetic theory seem to be the most accepted.

**2.1.1. The Free Volume Theory.** The free volume theory is based on a model developed by Eyring for molecular motions of small molecules. Eyring's model simply stated that in order for a molecule to move, a hole must be created for that molecule to move in.<sup>17</sup> This model was later modified to one that allowed a cooperative movement of molecules or polymer segments.<sup>18</sup> The model as proposed by Bueche asserted that in order for a polymer segment to move, a certain amount of energy must be localized on it and its neighboring segments. This energy would then be expended in creating a large enough free volume for the segmental motions to take place. The variation of specific volume with temperature for an amorphous polymer is such that its temperature-volume graph consists of two lines which intersect at the glass transition temperature. This is shown in Figure 2.1. The slopes of the lines are a measure of the thermal expansion coefficients,  $\alpha_G$  in the glassy state, and  $\alpha_L$  in the viscous or liquid state. The thermal

expansion coefficient is larger above the glass transition temperature than below it.<sup>19</sup> The difference in the expansion coefficients indicates the increased free volume above  $T_g$  and a consequent increase in segmental mobility. According to the model proposed by Bueche, the glass transition temperature can then be defined as the temperature at which polymer segments have gained enough energy and/or enough “room” for segmental motions to take place.<sup>20</sup> The relation between specific volume,  $v$ , and the glass transition temperature was expressed by Fox and Flory as;

$$v_g = v_{g\infty} - B(T_{g\infty} - T_g) \quad (1)$$

where  $v_g$  is the specific volume at  $T_g$ ,  $v_{g\infty}$  and  $T_{g\infty}$  are the limiting values at infinite polymer molecular weight, and  $B$  is a constant.<sup>21</sup> Simha and Boyer later studied a number of polymers and concluded that;

$$(\alpha_L - \alpha_G)T_g = K_1 \quad (2)$$

Simha and Boyer determined the constant  $K_1$  for a number of polymers as 0.113 and showed that Equation 2 held for a number of polymers regardless of variations in structures such as intermolecular forces, chain flexibility, and geometry.<sup>22</sup> This implied that the free volume at  $T_g$  was constant. Williams, Landel, and Ferry corroborated the concept of diminishing free volume by showing that the time required for segmental motions increased as the glass transition temperature was approached from higher temperatures.<sup>23</sup>

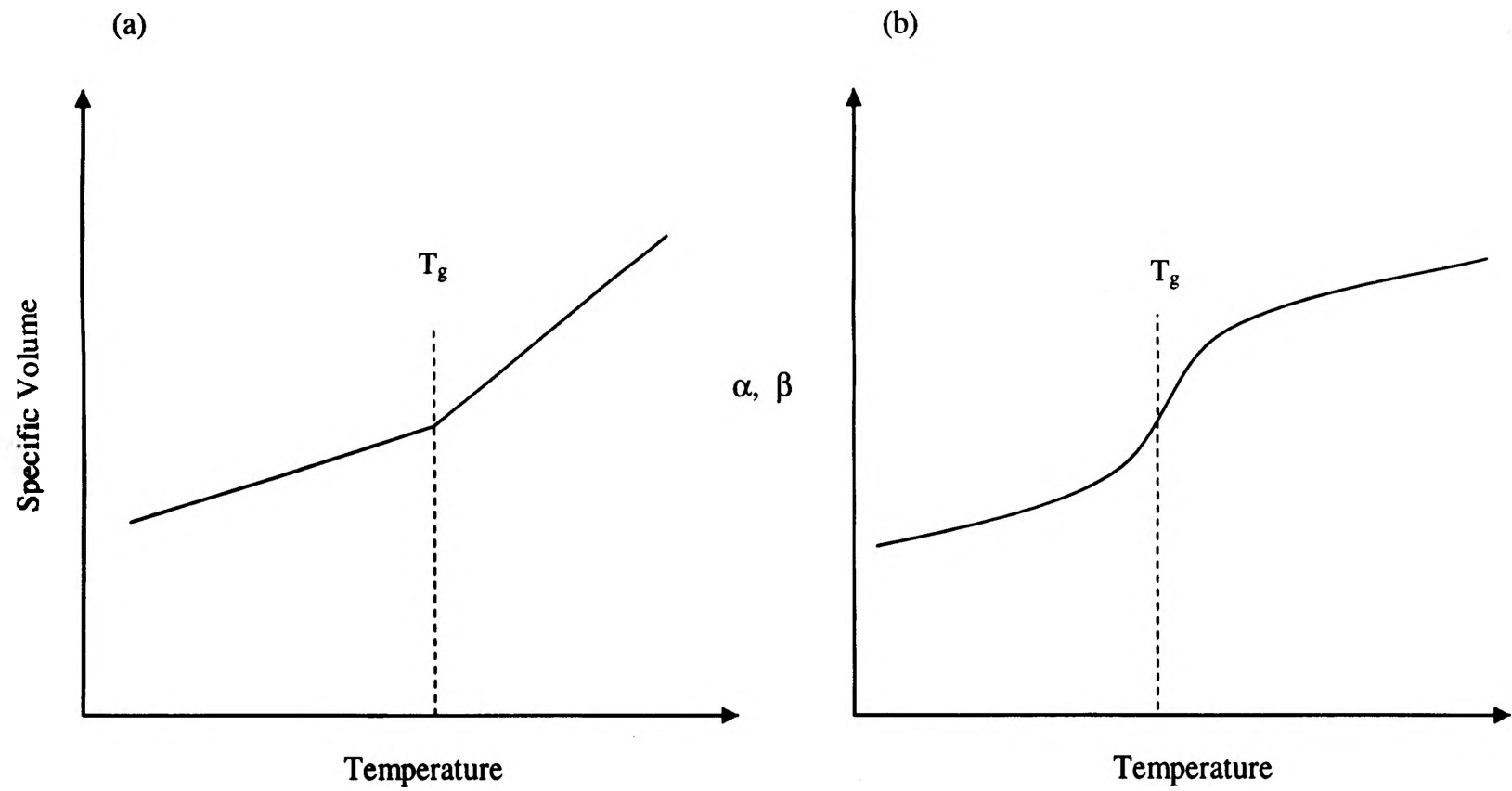


Figure 2.1. Variation of (a) specific volume, and (b) isothermal expansion coefficient,  $\alpha$ , and compressibility factor,  $\beta$ , with temperature.



They showed this by relating the viscosity of a polymer,  $\eta$ , at a temperature,  $T$ , above the  $T_g$  to the viscosity at  $T_g$  and the free volume in the WLF equation;

$$\ln\left(\frac{\eta}{\eta_g}\right) = -\frac{\frac{1}{f_g}(T - T_g)}{\frac{f_g}{\alpha_f} + (T - T_g)} \quad (3)$$

In this expression,  $f_g$  is the fractional free volume at  $T_g$  and  $\alpha_f$  is the difference between the thermal expansion coefficients above and below  $T_g$ . The value of  $f_g$  was determined as 0.025 and seemed to be constant for a number of polymers. This further supported the idea of an iso-free volume glass transition. The WLF equation for most linear, amorphous polymers is now widely accepted as;<sup>20</sup>

$$\log\left(\frac{\eta}{\eta_g}\right) = -\frac{17.44(T - T_g)}{51.6 + (T - T_g)} \quad (4)$$

**2.1.2. The Thermodynamic Theory.** The glass transition is often treated as a thermodynamic phenomenon because of the discontinuity in the coefficient of thermal expansion,  $\alpha$ , and the isothermal compressibility,  $\beta$ , (among others) at  $T_g$ , Figure 2.1. The glass transition is thought to be a second-order thermodynamic transition since these can be expressed as second derivatives of the Gibbs free energy,  $G$ ;<sup>20</sup>

$$\beta = -\frac{1}{V} \left( \frac{\partial V}{\partial P} \right)_T = -\frac{1}{V} \left( \frac{\partial^2 G}{\partial P^2} \right)_T \quad (5)$$

and

$$\alpha = \frac{1}{V} \left( \frac{\partial V}{\partial T} \right)_P = \frac{1}{V} \frac{\partial}{\partial T} \left( \frac{\partial G}{\partial P} \right)_T \quad (6)$$

Gibbs and DiMarzio used statistical mechanical calculations to show that there exists a second-order transition at a temperature,  $T_2$ , for amorphous linear polymers by showing that the second-order thermodynamic functions are discontinuous at  $T_2$ .<sup>24</sup> Their calculations also showed that the configurational entropy of the polymer was zero at the second-order transition temperature. The Gibbs-DiMarzio theory predicted an increase in the value of  $T_2$  with chain stiffness and polymer molecular weight, a decrease with increasing free volume and their results were in good agreement with experimental data. Gibbs and DiMarzio concluded that the  $T_2$  was the lower limit to the range of  $T_g$  at infinitely long experiments.

**2.1.3. The Kinetic Theory.** The thermodynamic theory of the glass transition assumes that the glass transition is an equilibrium process, but it has been shown that molecular relaxation times at and below  $T_g$  are way too long to permit a system to attain equilibrium on accessible timescales.<sup>25</sup> At temperatures way above  $T_g$ , the relaxation of most glass forming liquids following a small perturbation from metastable equilibrium (the linear dynamical response) has been shown to display single exponential behavior.

The linear response function,  $\phi$ , often takes the form;

$$\phi(t) = \exp\left(-\frac{t}{\tau}\right) \quad (7)$$

where  $t$  is the time. The temperature-dependent structural relaxation time,  $\tau$ , follows the Arrhenius expression  $\tau \sim \exp(E/kT)$  at temperatures above  $T_g$ .<sup>26</sup> Near  $T_g$  the structural relaxation of many structural glasses including polymers is non-exponential and follows the Kohlraush-Williams-Watts (KWW) function;<sup>27</sup>

$$\phi(t) = \exp\left[\left(-\frac{t}{\tau}\right)^\beta\right] \quad (8)$$

The exponent  $\beta$  is an indication of the width of a continuous relaxation time spectrum. At temperatures higher than  $T_g$ ,  $\beta \approx 1$  indicating a single-exponential relaxation. Around  $T_g$ ,  $\beta$  drops from unity to somewhere in the range 0.3-0.5 corresponding to a broad spectrum of relaxation times and a non-Arrhenius behavior of the relaxation times.<sup>26</sup> The non-Arrhenius pattern of the temperature dependence of relaxation times for polymers is often described by the Vogel-Tamman-Fulcher (VTF) equation;

$$\tau = \tau_0 \exp\left[\frac{E_0}{(T - T_0)}\right] \quad (9)$$

where  $\tau_0$ ,  $E_0$ , and  $T_0$  are temperature-independent parameters. The glass transition is thus viewed as a kinetic phenomenon that reflects a falling-out of equilibrium.<sup>26</sup>

The WLF equation elucidated the relation of free volume and the glass transition under the free-volume theory, but it also brings up the kinetic behavior of the glass transition. By noting that viscosity,  $\eta$ , is proportional to the product of density and time,  $\rho t$ , and that,

$$\frac{\eta_1}{\eta_2} = \frac{\rho_1 t_1}{\rho_2 t_2} \quad (10)$$

the WLF equation can be written as;

$$\log\left(\frac{t}{t_g}\right) = \log a_T = -\frac{17.44(T - T_g)}{51.6 + (T - T_g)} \quad (11)$$

since the variation of  $\rho$  with temperature is much less than the variation of  $\eta$ .<sup>20</sup> The equation shows that  $T_g$  would be different if the experiments were done at different time scales. The glass transition temperature increases with decreasing time frames.

**2.1.4. Factors that Influence  $T_g$ .** The three theories discussed above all associate the glass transition with the free volume of a material. The free-volume theory defines the  $T_g$  as the temperature at which polymer segments have gained enough “room”, through expanded free volume, for segmental motions to take place. Under the kinetic theory,  $T_g$  is defined as the temperature below which molecular relaxation times are much longer than the experimental time scales, and this decrease in relaxation times is due to a loss in configurational entropy because of free volume collapse. Thus any factor that affects the free volume of a material would affect its  $T_g$ .<sup>19</sup>

**2.1.4.1. Molecular Weight.** The most commonly used description for the molecular weight dependence of  $T_g$  was developed by Fox and Flory and is given by the Fox-Flory equation;

$$T_g = T_{g,\infty} - \frac{K}{M} \quad (12)$$

where  $T_{g,\infty}$  is the glass transition temperature of an infinite molecular weight polymer,  $K$  is a constant, and  $M$  is the polymer molecular weight.<sup>28</sup> The decrease in  $T_g$  with molecular weight is due to the increased free volume created by chain ends. A polymer of molecular weight  $M$  contains an extra free volume per cubic centimeters equal to  $\theta \left( \frac{2\rho N}{M} \right)$  compared to an infinite molecular weight polymer.<sup>18</sup>  $\theta$  is the free volume contributed by a chain end,  $\rho$  is the density, and  $N$  is Avogadro's number. The derivation of the Fox-Flory equation was based on the assumption that the glass transition occurs at a constant value of the free volume fraction, the iso-free volume theory. Fox and Flory reasoned that to compensate for the increasing free volume as polymer molecular weight decreased, a reduction in  $T_g$  was necessary in order to attain the constant free volume fraction.<sup>13</sup> Bueche used similar rationale and showed that;

$$T_g = T_{g,\infty} - \left( \frac{2\rho N\theta}{\alpha} \right) \frac{1}{M} \quad (13)$$

where  $\alpha$  is the free volume expansion coefficient and  $\alpha = \alpha_L - \alpha_G$ .<sup>19</sup> Turner extended this equation to include the effect of entanglements by noting that an extra amount of free volume is given off when entanglements are “released” as the molecular weight of polymers decreases.<sup>29</sup> He derived the expression;

$$T_g = T_{g,\infty} - \left( \frac{\rho N}{\alpha} \right) (\theta_1 + 2\theta_2) \left( \frac{1}{M} \right) \quad (14)$$

In this equation  $\theta_1$  designates the free volume given off when an entanglement is released and  $\theta_2$  denotes the free volume contributed by a chain end.

**2.1.4.2. Copolymerization.** The dependence of  $T_g$  on composition of random copolymers follows the Fox equation;

$$\frac{1}{T_g} = \frac{w_1}{T_{g1}} + \frac{w_2}{T_{g2}} \quad (15)$$

where  $w_1$  and  $w_2$  are the weight fractions of the two comonomers, and  $T_{g1}$  and  $T_{g2}$  designate the glass transition temperatures of the two corresponding homopolymers.<sup>30</sup> This equation predicts  $T_g$  values which are intermediate between the values of the homopolymers. For block and graft copolymers, two glass transitions corresponding to the respective homopolymers are usually observed.

**2.1.4.3. Cross-linking.** The introduction of cross-links into a polymer results in the reduction of the specific volume since van de Waals bonds are exchanged for shorter

and stronger primary bonds.<sup>21</sup> The relation of  $T_g$  to the degree of cross-linking in a polymer derived by Fox and Loshaek states that;

$$T_g = T_{g,\infty} - \frac{K}{M} + K_x \rho \quad (16)$$

In this equation,  $T_{g,\infty}$ ,  $K$ , and  $M$  all have the same meaning as used in the Fox-Flory equation for the variation of  $T_g$  with molecular weight.  $K_x$  is a constant and  $\rho$  is the number of crosslinks per gram.<sup>21</sup>

**2.1.4.4. Tacticity.** The effect of tacticity on  $T_g$  of vinyl polymers is mostly observed when one of the two carbons in the repeating unit has two dissimilar substituents and none of them being hydrogen, i.e., for polymers of the type  $(CH_2CXY)_n$  with  $X \neq Y \neq \text{hydrogen}$ . The  $T_g$  of syndiotactic isomers has been shown to be higher than their isotactic counterparts.<sup>31</sup> Karasz and MacKnight noted that this variation of  $T_g$  with tacticity is due to the greater energy difference between the two predominant rotamers for the syndiotactic configuration than the isotactic configuration.<sup>32</sup> After studying a series of poly(alkyl methacrylate)'s they concluded that for any syndiotactic-isotactic pair obeying the Simha-Boyer relation that the product  $\Delta\alpha T_g$  is constant, the difference in  $T_g$  can be predicted by the expression;

$$T_g(\text{syndiotactic}) - T_g(\text{isotactic}) = \frac{0.59\Delta\epsilon}{k} \quad (17)$$

where  $\Delta\epsilon$  is the difference in intramolecular or “flex” energy between the syndiotactic and isotactic isomers,  $k$  is the Boltzman constant.

**2.1.4.5. Plasticizers.** Plasticizers lower the  $T_g$  of polymers by increasing the free volume of the system. Kelley and Bueche developed a simple mathematical expression which describes the variation of  $T_g$  with plasticizer concentration.<sup>33</sup> The derivation was based on the assumption that the free volumes of the polymer and the plasticizer are additive and that the free volume of a material,  $V_f$ , at temperature  $T$  above  $T_g$  is given by;

$$V_f = 0.025 + \alpha(T - T_g) \quad (18)$$

If  $V_P$  and  $V_D$  are the volume fractions of polymer and diluent respectively in a plasticized polymer system, then assuming additivity of free volume, the total free volume of the system is given by;

$$V_f = V_P [0.025 + \alpha_P (T - T_{gP})] + V_D [0.025 + \alpha_D (T - T_{gD})] \quad (19)$$

which upon simplification leads to;

$$V_f = 0.025 + \alpha_P V_P (T - T_{gP}) + \alpha_D V_D (T - T_{gD}) \quad (20)$$

At  $T = T_g$ , the free volume  $V_f = 0.025$ . Substitution into Equation 20 followed by rearrangement gives the expression for the  $T_g$  of a plasticized polymer;<sup>33</sup>



$$T_g = \frac{\alpha_p V_p T_{gp} + \alpha_D (1 - V_p) T_{gD}}{\alpha_p V_p + \alpha_D (1 - V_p)} \quad (21)$$

The expression requires the knowledge of  $T_{gD}$  and  $\alpha_D$ , the  $T_g$  of the plasticizer and its free volume expansion coefficient, respectively, which are not usually available because of the difficulty in measuring them.<sup>31</sup>

## 2.2. ADSORPTION OF POLYMERS ON SURFACES

Polymers are used in a wide range of technologies and in most of these the adsorption of polymers plays a very important role. For example, in medicine polymers adsorb on artificial interfaces such as prosthetic implant. The formation of a paint film on a substrate proceeds via the adsorption of a polymer in the coating. The formation of glued joints includes the adsorption of polymers as the first stage.<sup>1</sup> The study of polymer adsorption is therefore of great importance to many technologies. Several techniques have been used to study the kinetics and equilibrium of adsorption. Most of these methods are similar to those used in studying the adsorption of non-polymeric molecules.<sup>1</sup> Ellipsometry has been used extensively in studying the thickness of polymer films.<sup>1</sup> Santore and Fu used total internal reflectance fluorescence to study the kinetics of competitive adsorption of poly(ethylene oxide) (PEO) chains with different molecular weights.<sup>34</sup> Nuclear magnetic resonance (NMR) spectroscopy has been used to study both the structure and dynamics of adsorbed polymers. Blum and Lin used deuterium NMR to probe the segmental dynamics of silica adsorbed poly(methyl acrylate)-d<sub>3</sub>.<sup>34</sup> Infrared spectroscopy has also found wide usage in the investigation of the adsorption of polymers, especially in determining bound fractions.

**2.2.1. Polymer Chain Conformations.** In most applications, polymers adsorb onto a solid surface from solution. The simplest model that describes the conformation of polymer molecules in solution is the random flight chain. In such a model a wide variety of different conformations are assumed to occur more or less randomly along the length of a polymer chain.<sup>20</sup> There are no restrictions on the torsional mobility of the polymer chain. For such a freely jointed chain, the mean-square-end-to-end distance is given by;

$$\langle r^2 \rangle^{\frac{1}{2}} = n^{\frac{1}{2}} l \quad (22)$$

where  $n$  is the number of segments and  $l$  is the length of each segment. The radius of gyration,  $\langle s^2 \rangle^{\frac{1}{2}}$ , which is the root mean square distance of an end from the center of gravity is related to the mean-square-end-to-end distance by;

$$\langle s^2 \rangle^{\frac{1}{2}} = \frac{1}{\sqrt{6}} \langle r^2 \rangle^{\frac{1}{2}} \quad (23)$$

Both  $\langle s^2 \rangle^{\frac{1}{2}}$  and  $\langle r^2 \rangle^{\frac{1}{2}}$  are dependent on the polymer molecular weight  $M$  and they have been shown to increase as  $M^{\frac{1}{2}}$ .<sup>36</sup>

This model falters when the fact that bonds formed along the polymer chain backbone have fixed bond angles and that the rotations of the C-C bond around another are not equally probable due to steric hindrance is taken into consideration. The

expression for the mean-square-end-to-end distance has been modified to compensate for these. The modified equation is;

$$\langle r^2 \rangle = nl^2 \left( \frac{1 - \cos \theta}{1 + \cos \theta} \right) \left( \frac{1 + \cos \phi}{1 - \cos \phi} \right) \quad (24)$$

where  $\theta$  is the bond angle and  $\phi$  is the bond rotational angle. The random flight model assumes that the polymer chain does not occupy any volume, i.e., the chain is infinitely thin.<sup>37</sup> But chain segments do occupy volume and consequently exclude others from occupying the same space.

The polymer coil dimensions  $\langle s^2 \rangle^{\frac{1}{2}}$  and  $\langle r^2 \rangle^{\frac{1}{2}}$  both depend on the nature of solvent. This dependence is expressed by the Flory-Huggins interaction parameter  $\chi$ . In a thermodynamically “good” solvent,  $\chi$  is close to zero and the polymer chains assume a spread out conformation.<sup>38</sup> Polymer-solvent interactions are more favorable than polymer-polymer and solvent-solvent interactions. In such solvents the size of the polymer chain increases as  $M^{\frac{3}{5}}$ . In a poor solvent there are greater attractions between the monomer units and the chain balls up. The chain dimensions in this condition scales as  $M^{\frac{1}{3}}$ . This is shown in Figure 2.2. There is a condition at which the polymer-solvent interactions and polymer-polymer interactions are equal called the theta condition. At the  $\theta$  point  $\chi = 0.5$  and the polymer chain behaves like an ideal chain.<sup>37</sup>

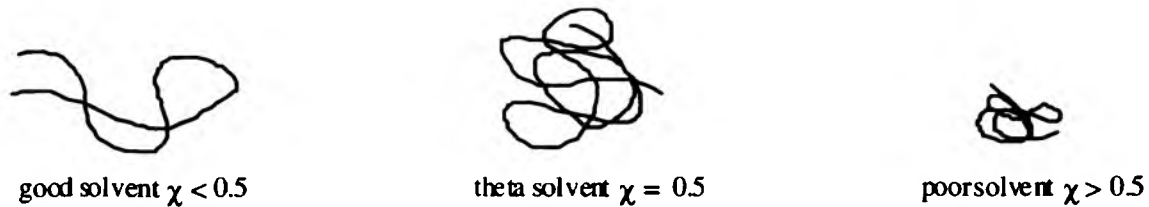


Figure 2.2. Effect of solvent on polymer chain dimensions.

**2.2.2. Driving Force for Adsorption.** Adsorption of a polymer molecule onto a solid surface result in the loss of conformational entropy as well as translational entropy for the polymer.<sup>39</sup> Thus, in the absence of any specific interactions between polymer segments and the surface, adsorption appears to be unfavorable. But for polymer adsorption from solution, a solvent molecule at a surface site is exchanged with a polymer segment. A dimensionless parameter  $\chi_s$  (analogous to the Flory-Huggins interaction parameter) is then defined as the net adsorption energy of a polymer molecule onto a solid;

$$\chi_s = \frac{U_1 - U_2}{kT} \quad (25)$$

where  $U_1$  and  $U_2$  are the adsorption energies of a solvent molecule and polymer segment, respectively,  $k$  is the Boltzman constant and  $T$  is the temperature.<sup>39</sup> A positive  $\chi_s$  (segment preferred over solvent molecule) provides the driving force for polymer adsorption. The critical adsorption energy  $\chi_{sc}$ , which is the minimum energy needed for

polymers to adsorb, has been shown to be of a few tenths of  $kT$  per segment.<sup>40</sup> The low  $\chi_{sc}$  results in the high affinity character of polymer adsorption.

**2.2.3. Formation of an Adsorbed Layer.** The rate of formation of an adsorbed layer is controlled by three processes, (i) transport of polymer molecules to the surface of the adsorbate by diffusion and convection, (ii) attachment of polymer on surface, and (iii) spreading of polymer chains to minimize their free energy.<sup>41</sup> The rate of transport of the polymers to the surface of adsorbate can be calculated precisely in simple cases where the system geometry and hydrodynamic conditions are well defined.<sup>41</sup>

For attachment, a common assumption is that attachment is very rapid on a bare surface and then slows down proportionally with increasing coverage.<sup>41</sup> The adsorbed amount,  $\Gamma$ , increases linearly with time and then asymptotes when the rate of adsorption is equal to the rate of desorption. The slope of the initial part of an adsorption isotherm for polymers depends largely on the diffusion coefficient and the concentration of the polymer.<sup>41</sup>

By the Langmiur adsorption isotherm equation, the rate of adsorption is given by;

$$R_{ad} = k_1 c(1 - \theta) - k_2 \theta \quad (26)$$

where  $k_1$  and  $k_2$  are the rate constants of adsorption and desorption, respectively,  $\theta$  is the fraction of surface covered with adsorbed polymers, and  $c$  is the concentration of the polymer in solution.<sup>42</sup> The fraction of the covered surface at varying concentrations can be determined by the expression;

$$\theta = 1 - \frac{c + k}{c_0 + k} \quad (27)$$

where  $c_0$  is the initial concentration of polymer in solution and  $k = \frac{k_2}{k_1}$ .<sup>42</sup>

Cohen Stuart and coworkers studied the effects of spreading in adsorption by probing the adsorption of a protein, immunoglobulin IgG, from aqueous solutions on silica.<sup>43</sup> They observed that at high polymer supply rate (to the adsorbate) the adsorbed amount reaches a maximum value and then decreases. Such an overshoot effect was not observed at low polymer concentrations (i.e. low supply rate). They rationalized that there was a surface process occurring in layers that are rapidly deposited that leads to desorption and that this process was spreading of the adsorbed polymer molecules. Pefferkorn and Elaisarri made similar observations in a different study.<sup>44</sup> The explanation given for these observations was that at low rate of supply individual chains have time to spread on the surface so that the surface gradually fills with spread molecules. The spreading relaxation time  $\tau_{ads}$  is given by;

$$\frac{\sigma - \sigma_{eq}}{\sigma_m - \sigma_{eq}} = \exp\left(-\frac{t}{\tau_{ads}}\right) \quad (28)$$

where  $\sigma_m$  is the macromolecular area at the initial time of contact with the surface and  $\sigma_{eq}$  the surface occupied by the isolated flat polymer in a thermodynamic equilibrium state.<sup>44</sup>

Spreading has profound effects on the amount of adsorbed polymer. As outlined above, at slow polymer supply to the surface each molecule has enough time to spread

before the surface is saturated. This results in a thin adsorbed layer.<sup>37</sup> Conversely, at fast supply, a thicker film is obtained since the molecules are surrounded by neighbors before they have time to spread. Figure 2.3 below shows the two cases.

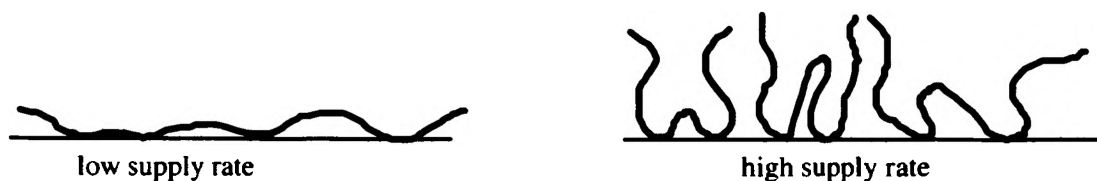


Figure 2.3. Spreading effects on adsorbed layer thickness.

**2.2.4. Conformation of the Adsorbed Layer.** When linear polymer molecules adsorb to a solid surface, three types of segment sequence are usually observed; trains, loops, and tails.<sup>41</sup>

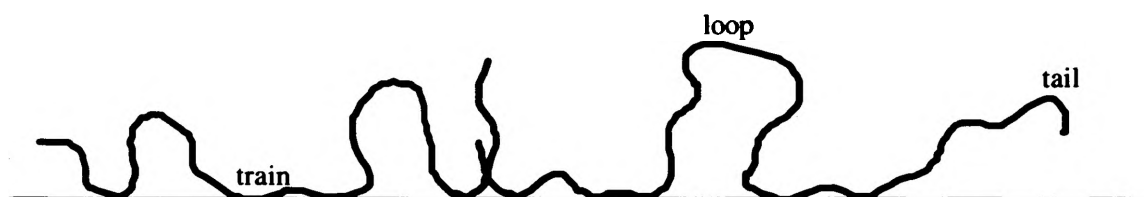


Figure 2.4. The loop-tail-train model of an adsorbed polymer.

Trains consist of a series of consecutive segments all in direct contact with the surface. A loop has no contact with the surface but is bound by trains on either side. Tails, which constitute a small proportion of all segments, are simply non-adsorbed chain ends bound

to a train.<sup>40</sup> Despite their low density, tails determine the hydrodynamic layer thickness  $\delta_h$  of the adsorbed polymer. Measurements and calculations shows that  $\delta_h$  is very small at low coverage but increases enormously as saturation is reached, and that the maximum layer thickness observed becomes strongly dependent on molecular weight.<sup>37</sup>

### 2.3. MODULATED DIFFERENTIAL SCANNING CALORIMETRY (MDSC)

Differential Scanning Calorimetry (DSC) is a thermal analysis technique used to measure the temperatures and heat flows associated with transitions in materials as a function of time and temperature.<sup>45</sup> Modulated Differential Scanning Calorimetry (MDSC) is a fairly new extension of DSC in which a sinusoidal perturbation is superimposed on the normal temperature scan used in DSC and the resultant data is deconvoluted by Fourier transformation. In the conventional heat-flux DSC, a sample and an inert reference are subjected to a linear heating/cooling scan and the difference in heat flow between the sample and the reference is measured as a function of time and temperature.<sup>45</sup> The temperature program in this case is given by;

$$T_t = T_o + \beta t \quad (29)$$

where  $T_t$  is the temperature at time  $t$ ,  $T_o$  is the starting temperature, and  $\beta$  is the heating rate. The total heat flow in DSC is made up of two components, one which is dependent on the heating rate and one which is a function of absolute temperature and time. This can be stated mathematically as;



$$\frac{dQ}{dT} = C_p \left( \frac{dT}{dt} \right) + f(T, t) \quad (30)$$

where  $\frac{dQ}{dT}$  is the differential heat flow rate,  $\frac{dT}{dt}$  is the heating rate, and  $C_p$  is the heat capacity. In MDSC the temperature program includes an additional term that accounts for the modulation;

$$T_t = T_o + \beta t + A \sin(\omega t) \quad (31)$$

$A$  is the amplitude of the temperature modulation and  $\omega$  is its frequency. When the amplitude is set to zero, Equation 31 will be the same as Equation 29 and so conventional DSC can be regarded as a special case of MDSC where the modulation has been turned off.<sup>46</sup> A temperature profile for an MDSC scan with a heating rate of 2.5 °C/min, a temperature modulation of  $\pm 1$  °C, and a period of 60 s is shown in Figure 2.5. Under these conditions, the instantaneous heating rate toggles between a high of 3.1 °C/min and a low of -1.1 °C/min. Thus the average temperature of the sample increases in a sinusoidal manner. It is this process that enables MDSC to estimate the individual contributions to the total heat flow by the heating rate dependent component and the absolute temperature and time dependent component.<sup>47</sup>

Thermal transitions which are dependent on the heating rate are termed “reversing” transition because they can be reversed by alternating heating and cooling. The glass transition and heat capacity are reversing. The heat flow associated with such transitions is called “reversing heat flow”. The “non-reversing heat flow” is due to

processes that are functions of absolute temperature and time only, and these include curing, evaporation, and decomposition.<sup>45</sup> The raw data of MDSC is complex (Figure 2.6) and Fourier transformation software is used to deconvolute the data. Figure 2.7 shows the MDSC heat flow, the reversing heat flow, and the non-reversing heat flow curves for a poly(methyl methacrylate) sample which exhibits a glass transition at 133 °C.

To obtain the reversing heat flow,  $C_p \left( \frac{dT}{dt} \right)$ , the value of  $C_p$  is determined from the quotient of the amplitudes of the heat flow and the modulated temperature using a Discrete Fourier Transformation.<sup>48,49</sup> The non-reversing heat is then taken as the difference of the total heat flow and the reversing heat flow.

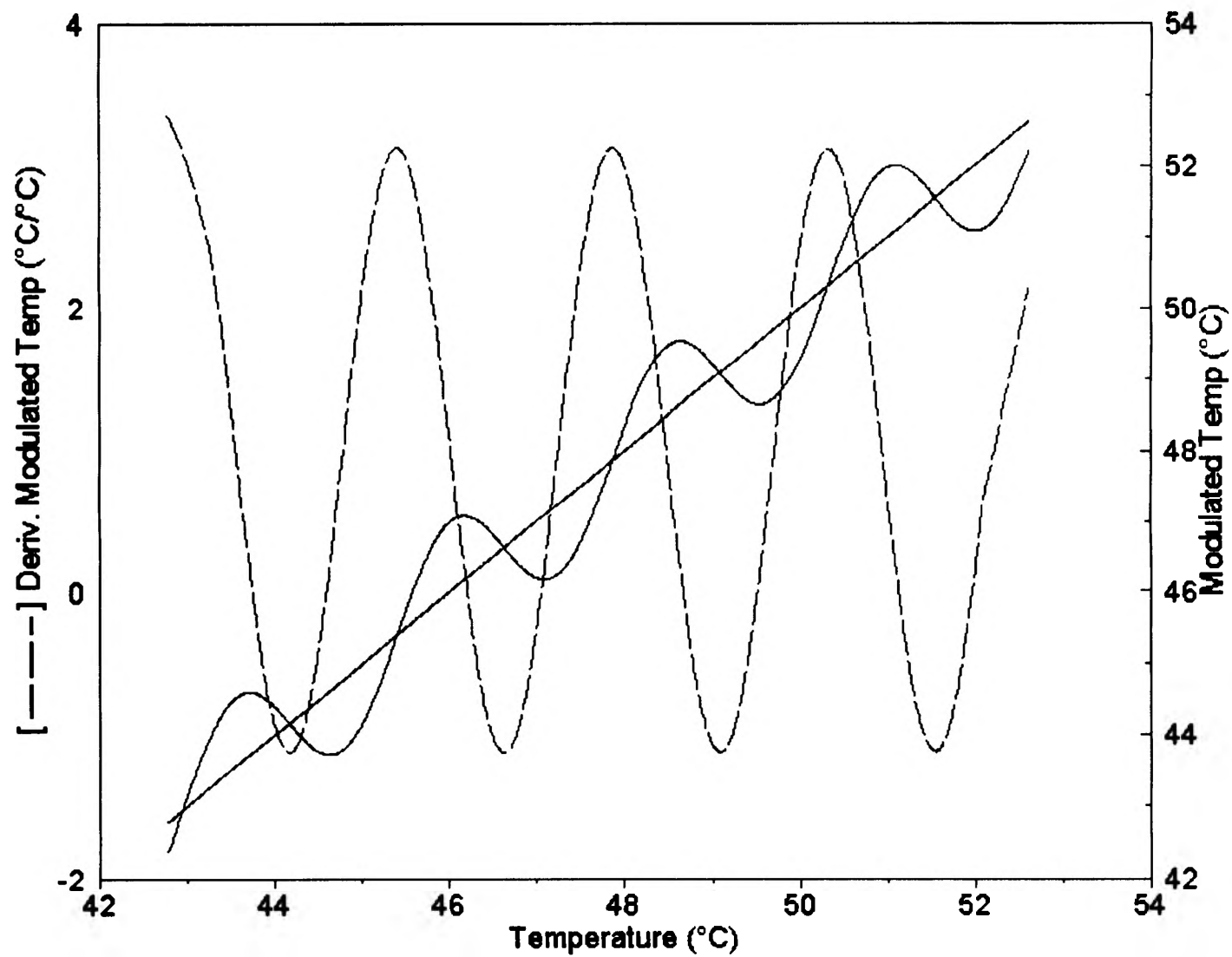


Figure 2.5. MDSC heating profile with an underlying heating rate of 2.5 °C/minute, a modulation period of 60 seconds, and a modulation period of  $\pm 1$  °C.

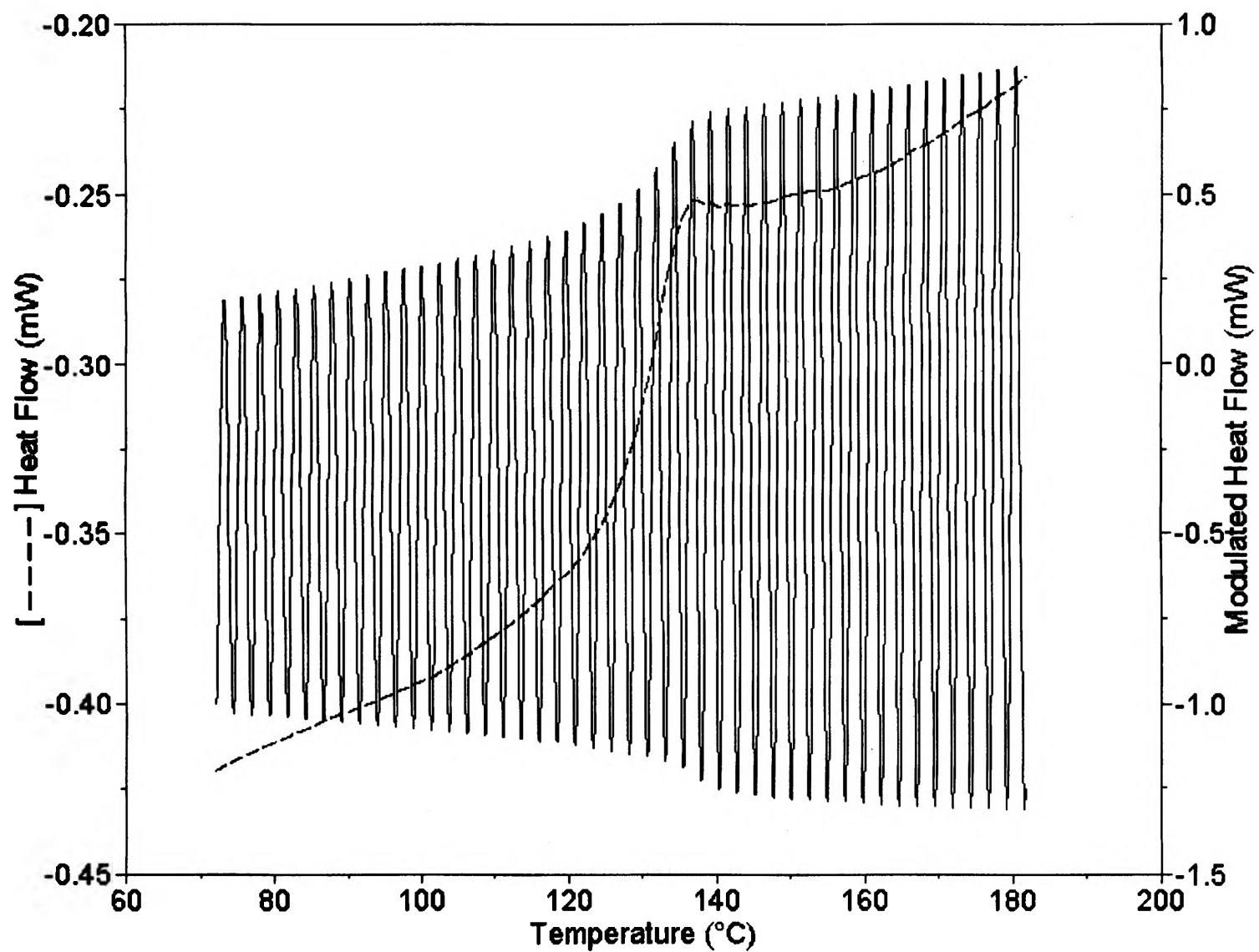


Figure 2.6. MDSC data for a PMMA sample showing the complex raw data and the deconvoluted heat flow curve.

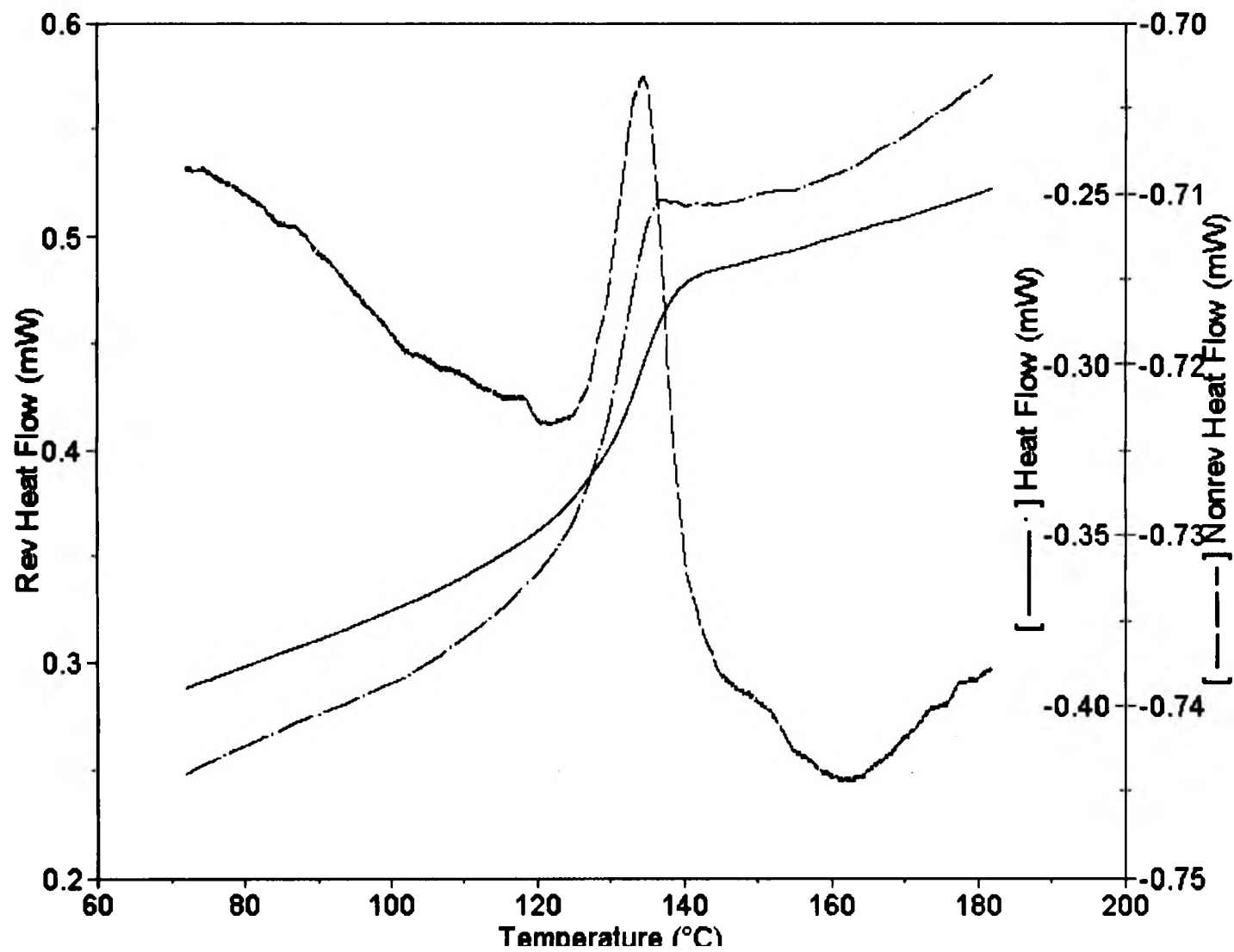


Figure 2.7. MDSC data for a PMMA sample showing the total heat flow and its two components, the reversing heat flow and the non-reversing heat flow.

## 2.4. REFERENCE

1. Lipatov, Y.; Sergeeva, L. M. *Adsorption of Polymers*; Halsted: New York, 1974.
2. Frank, C. W.; Rao, V.; Despotopoulou, M. M.; Pease, R. F. W.; Hinsberg, W. D.; Miller, R. D.; Rabolt, J. F. *Science* **1996** 273, 912.
3. Jones, R. A. L. *Current Opinion in Colloid and Interface Science* **1999**, 4, 153.
4. Lin, W.; Blum, F. D. *J. Am. Chem. Soc.* **2001**, 123, 2023.
5. Nasreddine, V.; Halla, J.; Reven, L. *Macromolecules* **2001**, 34, 7403.
6. Mirau, P. A.; Heffner, S. A. *Macromolecules* **1999**, 32, 4912.
7. Cho, Y.; Watanabe, H.; Granick, S. *J. Chem. Phys.* **1999**, 110, 9698.
8. Fukao, K.; Miyamoto, Y. *Phys. Chem Rev. E* **2000**, 61, 1743.
9. Tseng, K. C.; Turro, N. J.; Durning, C. J. *Phys. Chem. Rev. E* **2000**, 61, 1800.
10. Frank, B.; Gast, A. P.; Russell, T. P.; Brown, H. R.; Hawker, C. *Macromolecules* **1996**, 29, 6531.
11. Tate, R. S.; Fryer, D. S.; Pasqualini, S.; Montague, M. F.; de Pablo, J. J.; Nealey, P. F. *J. Chem. Phys.* **2001**, 115, 9982.
12. Grohens, Y.; Sacristan, J.; Hamon, L.; Reinecke, H.; Mijangos, C.; Guenet, J. M. *Polymer* **2001**, 42, 6419.
13. Tsui, O. K. C.; Russell, T. P.; Hawker, C. J. *Macromolecules* **2001**, 34, 5535.
14. Rohling, J. H.; Caldeira, A. M. F.; Pereira, J. R. D.; Medina, A. N.; Bento, A. C.; Baesso, M. L.; Miranda, L. C. M.; Rubira, A. F. *J. App. Phys.* **2001**, 89, 2220.
15. Gorbunov, V. V.; Fuchigama, N.; Tsuruk, V. V. *High Perform. Polym.* **2000**, 12, 603.
16. Fryer, D. S.; Nealey, P. F.; de Pablo, J. J. *J. Vac. Sci. Technol. B* **2000**, 18, 3376.
17. Eyring, H. *J. Chem. Phys.* **1936**, 4, 283.

18. Bueche, F. J. *Chem. Phys.* **1953**, *21*, 1850.
19. Bueche, F. *Physical Properties of Polymers*; Interscience Publishers: New York London, 1962.
20. Hiemenz, P.C. *Polymer Chemistry*; Marcel Dekker: New York, 1984.
21. Fox, T.G.; Loshaek, S. *J. Polymer Sci.* **1955**, *15*, 371.
22. Simha, R.; Boyer, R.F. *J. Chem. Phys.* **1962**, *37*, 1003.
23. Williams, M. L.; Landel, R. F.; Ferry, J. D.; *J. Am. Chem. Soc.*, **1955**, *77*, 3701.
24. Gibbs, J.H.; DiMarzio, E. U. *J. Chem. Phys.* **1958**, *28*, 373.
25. Adam, G.; Gibbs, J. H. *J. Chem. Phys.*, **1965**, *43*, 139.
26. Fredrickson, G. H. *Ann. Rev. Phys. Chem.* **1988**, *39*, 149.
27. Privalko, V. P. *J. Non-Cryst. Solids* **1999**, *255*, 259.
28. Sperling, L. H. *Introduction to Physical Polymer Chemistry*; 2<sup>nd</sup> Edition; Wiley-Interscience: New York, 1992.
29. Turner, D.T. *Polymer* **1978**, *19*, 789.
30. Fox, T. G. *Bull. Am. Phys. Soc.* **1956**, *1*, 123.
31. Eisenberg, A. in *Physical Properties of Polymers*; 2<sup>nd</sup> Edition; American Chemical Society: Washington, DC, 1993. Chapter 2.
32. Karasz, F. E.; MacKnight, W. J. *Macromolecules* **1968**, *1*, 537.
33. Kelley, F. N.; Bueche, F. J. *Polym. Sci.* **1961**, *50*, 549.
34. Santore, M.; Fu Z., *Macromolecules* **1997**, *30*, 8516
35. Blum, F. D.; Lin, W. *Macromolecules* **1998**, *31*, 4135.
36. Sun, S. F. *Physical Chemistry of Macromolecules*; John Wiley and Sons: New York, 1994.

37. Cohen Stuart M.A. *Surfactant Sci. Ser.* **1998**, 75, 1.
38. Rosen, S. L. *Fundamental Principles of Polymeric Materials*; John Wiley and Sons: New York, 1993.
39. Richards, R.W.; Jones R. A. L. *Polymers at Surfaces and Interfaces*; Cambridge University Press: New York, 1999.
40. Partiff, G. D.; Rochester, C. H. (Eds.) *Adsorption from Solution at the Solid/Liquid Interface*; Academic Press: London, New York, 1983.
41. Fleer, G. J.; Cohen Stuart, M. C.; Scheutjens, J. M.; Cosgrove, T.; Vincent, B. *Polymers at Interfaces*; Chapman and Hall: London, 1993.
42. Bajpai, U. D. N.; Bajpai A. K., *Polymer International* **1993**, 32, 43.
43. Cohen Stuart, M. A.; van Eijk, M. C. P.; Djit J. C.; Hoogeveen, G. N. *Macromol. Symp.* **1997**, 113, 163.
44. Pefferkorn E.; Elaissari A. *J. Colloid Interface Sci.* **1990**, 138, 187.
45. Gill, P. S.; Sauerbrunn, S. R.; Reading, M. *J. Thermal Anal.* **1993**, 40, 931.
46. Cao, J. *Thermochim. Acta* **1999**, 325, 101.
47. TA Instruments *Modulated DSC™ Compendium – Basic Theory and Experimental Considerations*; TA Instruments.
48. Reading, M. *J. Therm. Anal. Cal.* **2001**, 64, 7.
49. Reading M.; Luget, A.; Wilson, R. *Thermochimica Acta* **1994**, 238, 295.



### **3. MDSC AND FTIR STUDY OF THE GLASS TRANSITION OF POLY(METHYL METHACRYLATE) ADSORBED ON SILICA**

#### **3.1. ABSTRACT**

The glass transition behavior of poly(methyl methacrylate) (PMMA) thin films supported on silica was studied using modulated differential scanning calorimetry (MDSC). To vary the interaction between the polymer and substrate, two grades of silica were used: fumed amorphous silicon oxide, and fumed amorphous silicon oxide treated with hexamethyldisilazane (HMDS). The results presented here indicate that the glass transition of PMMA films on silicon oxide broadened significantly to temperatures above the bulk glass transition temperature,  $T_g$ . For PMMA films on silicon oxide treated with HMDS, no significant broadening in the glass transition was observed. The overall glass transition temperature for the PMMA films on untreated silica increased with decreasing adsorbed amount. Fourier Transform Infrared (FTIR) spectroscopy was used to show that the change in the  $T_g$  of the adsorbed polymers with adsorbed amount is due to the change in the configuration of the polymer chains. It was observed that the fraction of polymer segments in contact with the substrate decreased with increasing adsorbed amount.

#### **3.2. INTRODUCTION**

Due to miniaturization of devices in which polymer thin films are incorporated, the dynamics of polymer thin films has become increasingly important in the last decade. A number of techniques have been used to probe the dynamics of polymer thin films by studying the glass transition behavior of the films. In general, the behavior of polymers in these thin films is different from bulk behavior. The glass transition temperature,  $T_g$ , of

polymer thin films has been shown to vary with tacticity,<sup>1</sup> strength of the interaction between the polymer and substrate,<sup>2,3</sup> and film thickness.<sup>4-8</sup>

Ellipsometry and X-ray reflectivity have been used quite extensively in the study of polymer thin films.<sup>2,3,5,7</sup> In these techniques, the  $T_g$  of thin films is detected by the discontinuity in the thermal expansivity of the film.<sup>8</sup> The thermal expansion behavior of supported polystyrene films also has been studied by positron lifetime spectroscopy.<sup>9</sup> The dynamics of polymer thin films have been studied more directly by  $^2\text{H}$  NMR<sup>10</sup> and recently by  $^1\text{H}$  NMR with fast magic angle spinning.<sup>11</sup> The insensitivity of NMR and the strong dipolar interactions of protons have for a long time rendered  $^1\text{H}$  NMR an unlikely technique for the study of polymer interfaces. These limitations have been circumvented by isotopic labeling, spinning the sample at the magic angle, and performing the experiments at temperatures above the  $T_g$  of the polymer.<sup>11</sup>

The dynamics of the  $\alpha$  and  $\beta$  processes of thin films of poly(methyl methacrylate) (PMMA), poly(vinyl acetate) (PVAc), and polystyrene have been investigated by dielectric relaxation spectroscopy.<sup>12,13</sup> The  $T_g$  was determined as the temperature at which the temperature dependence of capacitance changed discontinuously. A fairly new technique, called Local Thermal Analysis (L-TA), has been used to probe the glass transition temperature for thin polymer films.<sup>14</sup> A thermal probe, mounted on a scanning probe microscope head, is brought in contact with a polymer film and its temperature is ramped from ambient temperature to temperatures above the  $T_g$  of the polymer. The combination of L-TA with near-field microscopy makes up micro-thermal analysis ( $\mu\text{TA}$ ).<sup>15</sup> In both these techniques, individual regions of a sample are selectively characterized with very little or no alteration to the rest of the sample.<sup>16</sup>

In this paper, we present the glass transition behavior of PMMA thin films adsorbed on silica using temperature-modulated differential scanning calorimetry (MDSC). Conventional DSC measures the difference in heat flow between a sample and reference as both the sample and reference are subjected to a linear heating profile. In MDSC, the linear heating ramp is modulated sinusoidally.<sup>17</sup> By using two heating profiles, MDSC gives a measure of the individual contributions of the reversing heat flow and the non-reversing heat flow to the total heat flow. The linear heating profile gives information on kinetic processes while the cyclic heating profile gives heat capacity information.<sup>18</sup> It has been shown that the high sensitivity of MDSC makes it possible to probe very thin films of polymers adsorbed on silica<sup>19</sup> and that MDSC can detect overlapping transitions as long as they are at least 5 °C apart.<sup>17</sup> We used MDSC to show that the glass transition of thin films of PMMA adsorbed on silica broadens to high temperatures and is a continuum of glass transition temperatures from polymer segments with different segmental mobilities. FTIR was used to estimate the bound fraction,  $p$ , the fraction of segments in contact with the substrate.

### 3.3. EXPERIMENTAL

**Materials.** Predominantly syndiotactic poly(methyl methacrylate) (PMMA) samples of narrow polydispersities (Polymer Source, Quebec, Canada) were used. Their properties are summarized in Table 3.1. The polydispersities were taken to be as specified by the manufacturer. Amorphous fumed silica (Cab-O-Sil M5, Cabot Corp.) with a manufacturer specified surface area of 200 m<sup>2</sup>/g and silica treated with

hexamethyldisilazane (HMDS) (Cab-O-Sil TS530) were used for the adsorption. Toluene (HPLC grade, Fisher Scientific) was used as obtained.

**Adsorption.** 10 mL PMMA solutions of concentrations 5 mg/mL and 10 mg/mL were prepared for each polymer sample. Adsorption was obtained by agitating 20mL capped glass tubes containing 300 mg of silica and the 10 mL polymer solution at room temperature for 48 h. The resulting suspension was centrifuged and the concentration of unabsorbed polymer remaining in the supernatant was determined by gravimetric analysis. The polymer-silica gel was dried for 3 days at room temperature and then under vacuum at 70 °C for 24 h. The final adsorbed amount was verified by thermogravimetric analysis, TGA, using a Hi-Res™ TGA 2950 Thermogravimetric Analyzer (TA Instruments, New Castle, DE).

**Characterization.** A DSC 2920 Modulated DSC™ (TA Instruments, New Castle, DE) was used to measure the glass transition temperature of the bulk and silica adsorbed PMMA samples. Sample masses of about 8 – 12 mg were used. Silica was used as the reference in the reference pan. Two heating scans and one cooling scan were taken from 25 to 280 °C, at a rate of 2.5 °C/min, and a modulation amplitude of 1 °C every 60 s. The sample cell was purged with N<sub>2</sub> gas at a flow rate of 50 ml/min during the scans. The first scan ensured that all samples were subjected to the same sample history and the reported glass transition temperatures are based on the second scan.

A Nicolet Magna-IR™ Spectrometer 750 (Nicolet Analytical) was used to record the FTIR data of the adsorbed polymers. A slurry of the silica-adsorbed PMMA (ca. 12 mg of silica-adsorbed PMMA in ca. 3 mL of toluene) was cast on a KBr cell and dried first at room temperature followed by vacuum oven drying at 70 °C for 1 hr. To get good

signal-to-noise ratios, 1024 scans were performed. Curve fittings on the acquired FTIR data was done using a Grams/32 AI software and the decomposition of the  $\nu(\text{CO})$  band suggested by Berquier and Arribart.<sup>20</sup>

### 3.4. RESULTS AND DISCUSSION

MDSC was performed to investigate the glass transition behavior of PMMA thin films adsorbed on silica. Varying the adsorbed amounts of the PMMA samples of different molecular weights made it possible to simultaneously test the effect of molecular weight and the adsorbed amount on the  $T_g$ . The bulk  $T_g$ 's of the polymers used in this study are in the range 116 to 133 °C and all have a transition breadth of ca.10 °C. The increase in  $T_g$  with molecular weight is expected and it reflects the increased ease of motion for low molecular weight polymers.<sup>21</sup> MDSC curves of the PMMA samples in bulk are shown in Figure 3.1. For simple, narrow transitions like these, the  $T_g$  is taken as the maximum of the differential of the reversing heat flow signal. The derivative mode is used here to highlight the complex behavior of glass transitions for the adsorbed polymers. The MDSC curves for the PMMA samples adsorbed on M5 (untreated silica) are shown in Figures 3.2-3.4. The glass transitions for the adsorbed polymers are much broader and more complex than the bulk glass transition. While it is convenient, to simply take the  $T_g$  of these samples as the peak maxima is not sufficient to describe the glass transition behavior because of the complexity of the  $T_g$  curves. The glass transitions for the adsorbed PMMA samples spans the 120 to 200 °C range, but have more intensity in the high temperature side. This indicates that a high fraction of polymers in the samples have higher  $T_g$ 's compared to bulk.

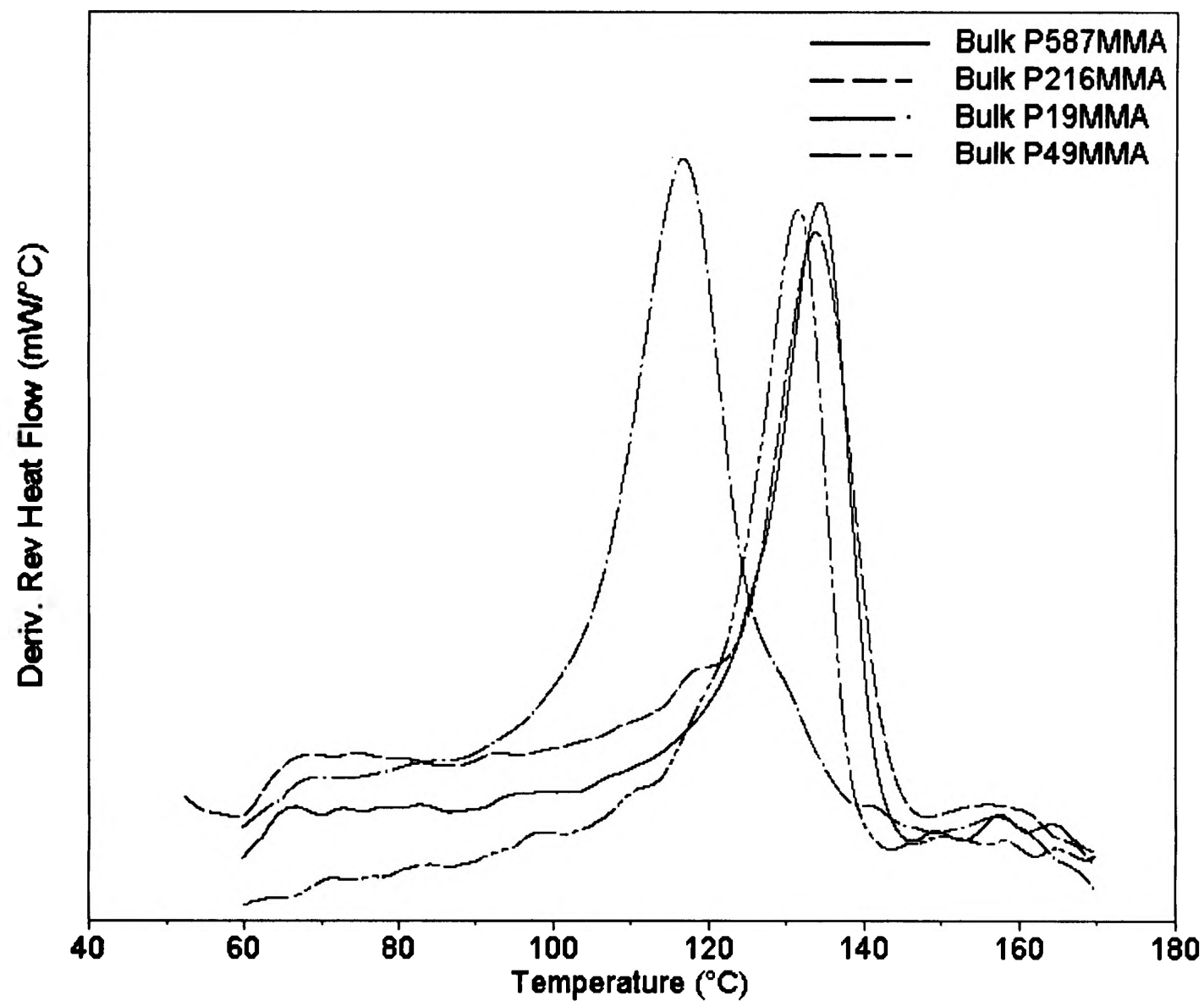


Figure 3.1. MDSC curves (derivative of the reversing heat flow) of bulk PMMA samples. The  $T_g$ 's are taken as the peak maxima.

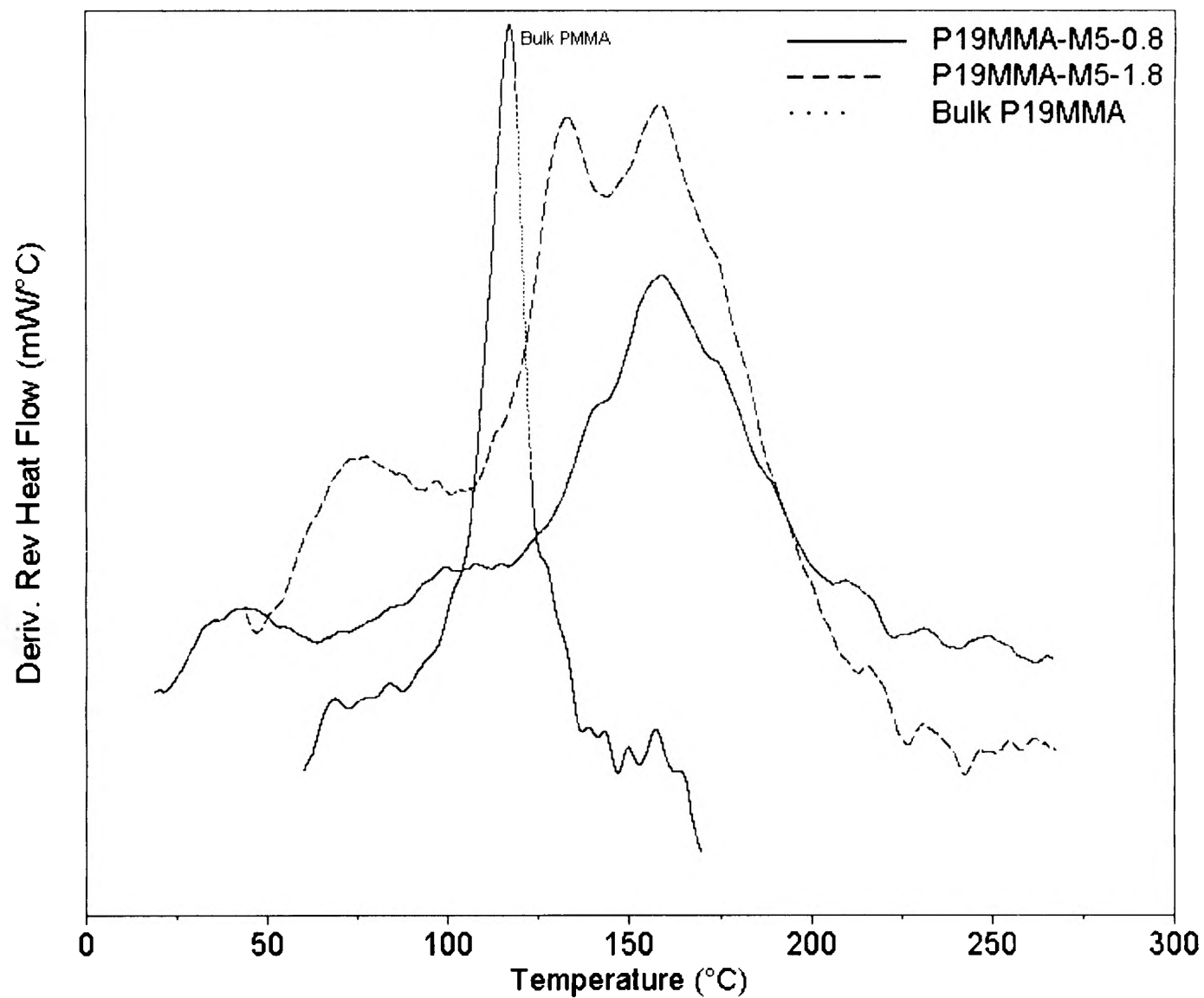


Figure 3.2. MDSC curves of bulk P19MMA and P19MMA adsorbed on M5 from 5 mg/mL (solid) and 10 mg/mL (dash) solutions.

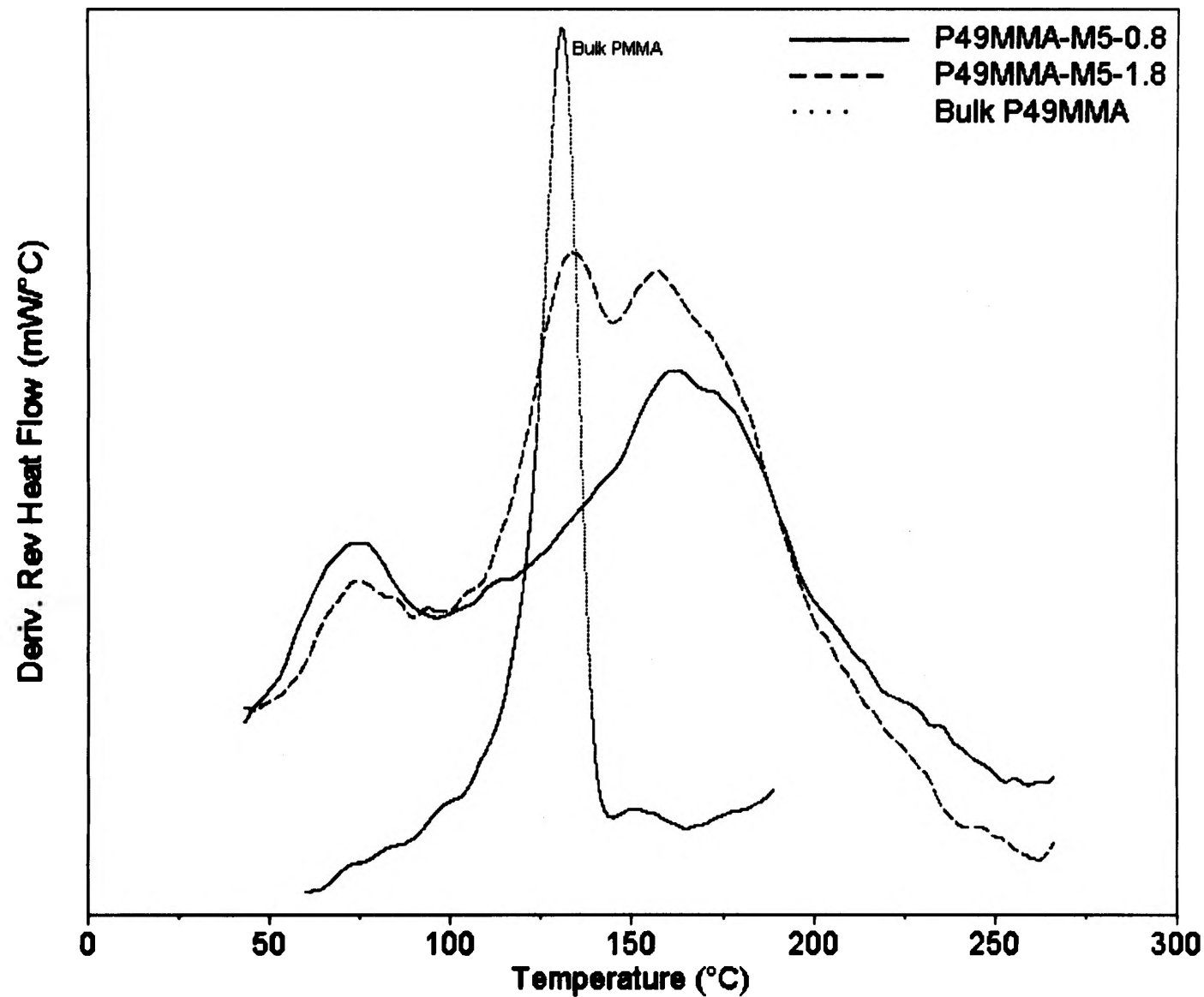


Figure 3.3. MDSC curves of bulk P49MMA and P49MMA adsorbed on M5 from 5 mg/mL (solid) and 10 mg/mL (dash) solutions.



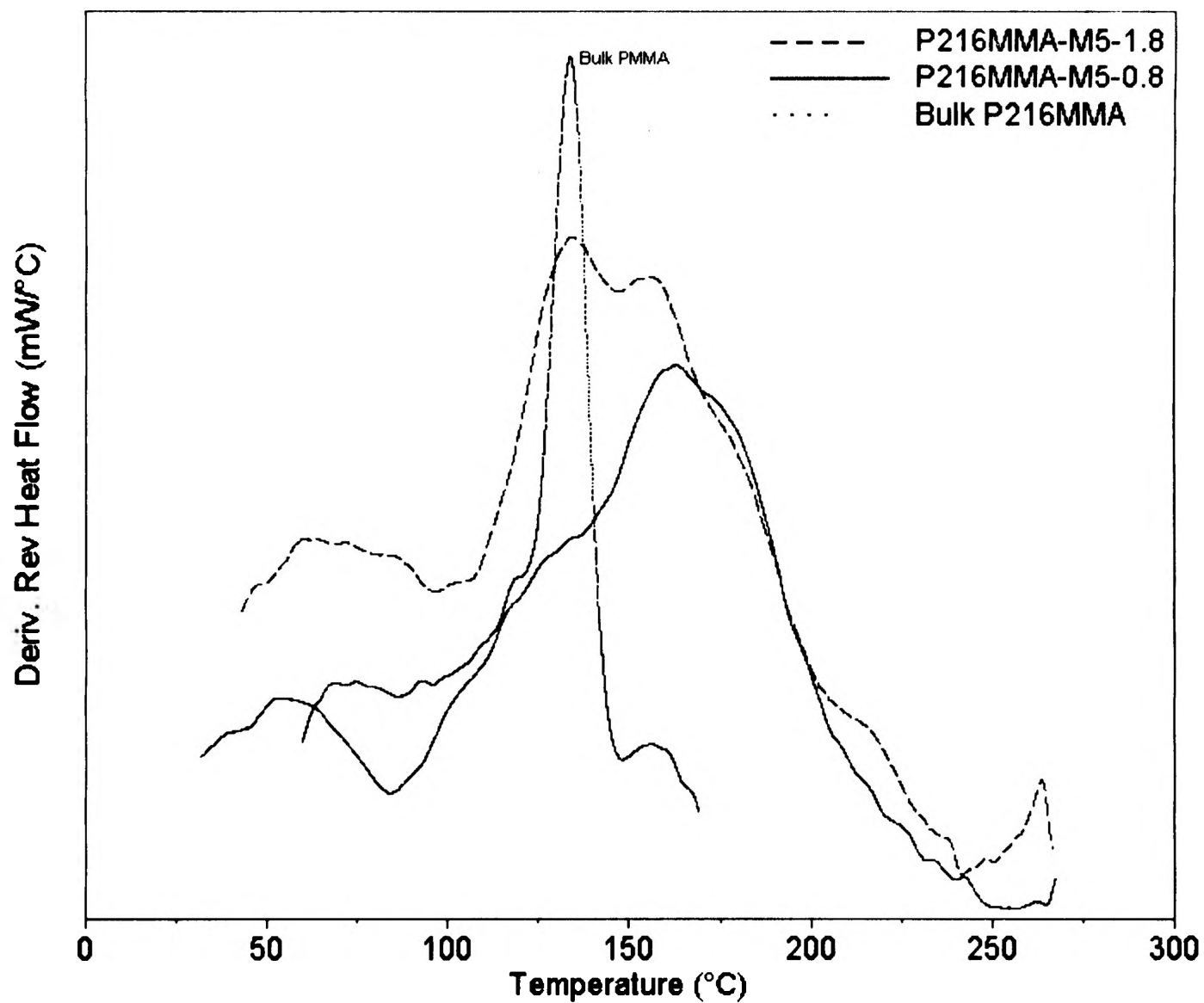


Figure 3.4. MDSC curves of bulk P216MMA and P216MMA adsorbed on M5 from 5 mg/mL (solid) and 10 mg/mL (dash) solutions.

Table 3.1. Polymer Samples of Poly(methyl methacrylate)

Sample	$M_w$ ( kg/mol)	$M_w/M_n$	Bulk $T_g$ (°C)	Transition Width (°C)
P19MMA	19.3	1.06	116	12
P49MMA	49.4	1.05	130	11
P216MMA	216	1.05	133	10
P587MMA	587	1.11	133	10

Table 3.2 shows the “ $T_g$ ’s” and transition breadths of the polymer thin films. Increases in  $T_g$  for PMMA adsorbed on silica substrates have been observed previously and were attributed to restricted segmental motion due to H-bonding between the carbonyl on PMMA and the surface hydroxyl groups.<sup>2,19</sup> Porter and Blum suggested that the broadened transition breadth was indicative of a motional gradient.<sup>19</sup> Polymer segments at the polymer-substrate interface are more restricted and have higher  $T_g$ ’s than segments not in contact with the substrate. The glass transition behavior of supported polymer thin films have received significant attention lately and there appears to be a consensus that the  $T_g$  of polymer films can either be depressed or elevated from the bulk value depending on the polymer-substrate interaction.<sup>8</sup> Such an observation was made by Keddie, Jones, and Cory when they measured the thickness dependence of the  $T_g$  of PMMA films adsorbed on silica and gold.<sup>2</sup> They observed a decrease in  $T_g$  with film thickness for the gold-adsorbed PMMA but a slight increase for PMMA films on silica. The rationale given for these observations was that there existed a liquid-like layer with enhanced mobility at the polymer-air interface and that this free surface effect was outweighed by the effect of H-bonding for PMMA adsorbed on silica. The same group had earlier observed a decrease in the  $T_g$  of thin polystyrene films on silicon wafers.<sup>22</sup> But Wallace *et al.* observed increased  $T_g$ ’s for PS films below 400 Å on hydrogen-terminated silicon substrate.<sup>23</sup> They concluded that the differences in their results and those of Keddie *et al.* were due to differences in the interactions of polymer and substrate. Strong adhesive forces between polymer and substrate would result in increased  $T_g$ .

Table 3.2. Thermal Characterization of the PMMA thin films adsorbed from 0.5%  
toluene solutions.

Sample	T <sub>g</sub> (°C)	Transition Width (°C)
P19MMA-0.8	160	50
P49MMA-0.8	164	55
P216MMA-0.8	164	54
P587MMA-0.8	163	53

Jones and Kawana have recently shown that the  $T_g$  of thin polystyrene films on silica substrates does not simply decrease but the transition broadens in the direction of lower temperatures.<sup>24</sup> They proposed that the broadening of the glass transition was due to heterogeneity in mobility properties. The glass transitions of the PMMA films studied in this work behave in a similar, though opposite, manner. This behavior is probably due to the strong PMMA-silica interactions, and we observe a broadening of the glass transition towards higher temperatures.

When the adsorbed amount was increased from 0.8 to ca. 1.8 mg/m<sup>2</sup>, the MDSC curves broadened and showed more intensity in the lower temperatures. Whereas a single broad peak was observed for the glass transition of the low adsorbed amount samples, Figures 3.2-3.4 and Table 3.3 show that the MDSC curves of the high-adsorbed amount samples have a second peak centered around 135 °C. The emergence of this peak in the lower temperature end of the surface glass transitions (120 – 200 °C) indicates that there is a higher fraction of segments not in contact with the surface for the high-adsorbed amount samples. This is in agreement with the Scheutjens-Fleer theory, which predicts a decrease in the bound fraction, the fraction of segments in contact with the surface, with increasing adsorbed amount and molecular weight. A high bound fraction corresponds to a flatter chain conformation, whereas a lower bound fraction is indicative of an adsorbed layer with long loops and tails.<sup>25</sup> Reading *et al.* used MDSC to determine the weight fraction of interface and the extent of phase separation in multi-component polymers.<sup>26</sup> The determination of weight fractions was based on the assumption that the interface could be modeled as a series of discrete fractions each with its own glass transition temperature. We believe that our system fits this model but we can unambiguously

Table 3.3. Thermal Characterization of the PMMA thin films adsorbed from 1% toluene solutions.

Sample	T <sub>g</sub> (°C)	Transition Width (°C)
P19MMA-1.8	132, 159	63
P49MMA-1.8	133, 160	67
P216MMA-1.8	134, 159	68
P587MMA-1.8	136, 156	68

identify two fractions only, a fraction at the polymer-substrate interface with restricted segmental mobility and a fraction with higher mobility at the polymer-air interface.

To investigate the change in polymer chain configuration as the adsorbed amount was varied, FTIR spectroscopy was used to estimate the bound fractions. When PMMA adsorbs on silica, the carbonyl band shifts to lower frequencies due to the formation of H-bonds.<sup>19,27</sup> The bound fraction can then be determined by separating the unperturbed and H-bonded carbonyl frequencies by curve fittings.<sup>29</sup> FTIR spectra of the adsorbed PMMA samples are shown in Figures 3.5-3.8. The unperturbed carbonyl band is centered around  $1735\text{ cm}^{-1}$  and the H-bonded carbonyl band appears as a shoulder around  $1711\text{ cm}^{-1}$ . We used the method for carbonyl band decomposition and estimation of bound fraction described by Berquier and Arribart.<sup>19</sup> The bound fractions are shown in Table 3.4. Figures 3.5-3.8 and Table 3.4 show that the bound fractions decreased with increasing adsorbed amount; from ca. 0.45 at  $0.8\text{ mg/m}^2$  to ca. 0.35 at  $1.8\text{ mg/m}^2$  indicating an increase in the fraction of more mobile segments. These results corroborate the MDSC results.

Although the adsorbed amount of polymers is known to increase with polymer molecular weight,<sup>25</sup> adsorption from 5 mg/mL PMMA solutions yielded similar adsorbed amounts for the different molecular weights as shown in Table 3.3. This suggests that for this polymer-solvent-substrate system, surface saturation (which varies with molecular weight) occurs at polymer concentrations equal to or above 5 mg/mL. Our results indicate that below surface saturation, polymers of different molecular weights assume rather flat conformations with similar bound fractions. This seems rather unlikely taking into consideration the larger entropy loss upon adsorption of the high molecular weight

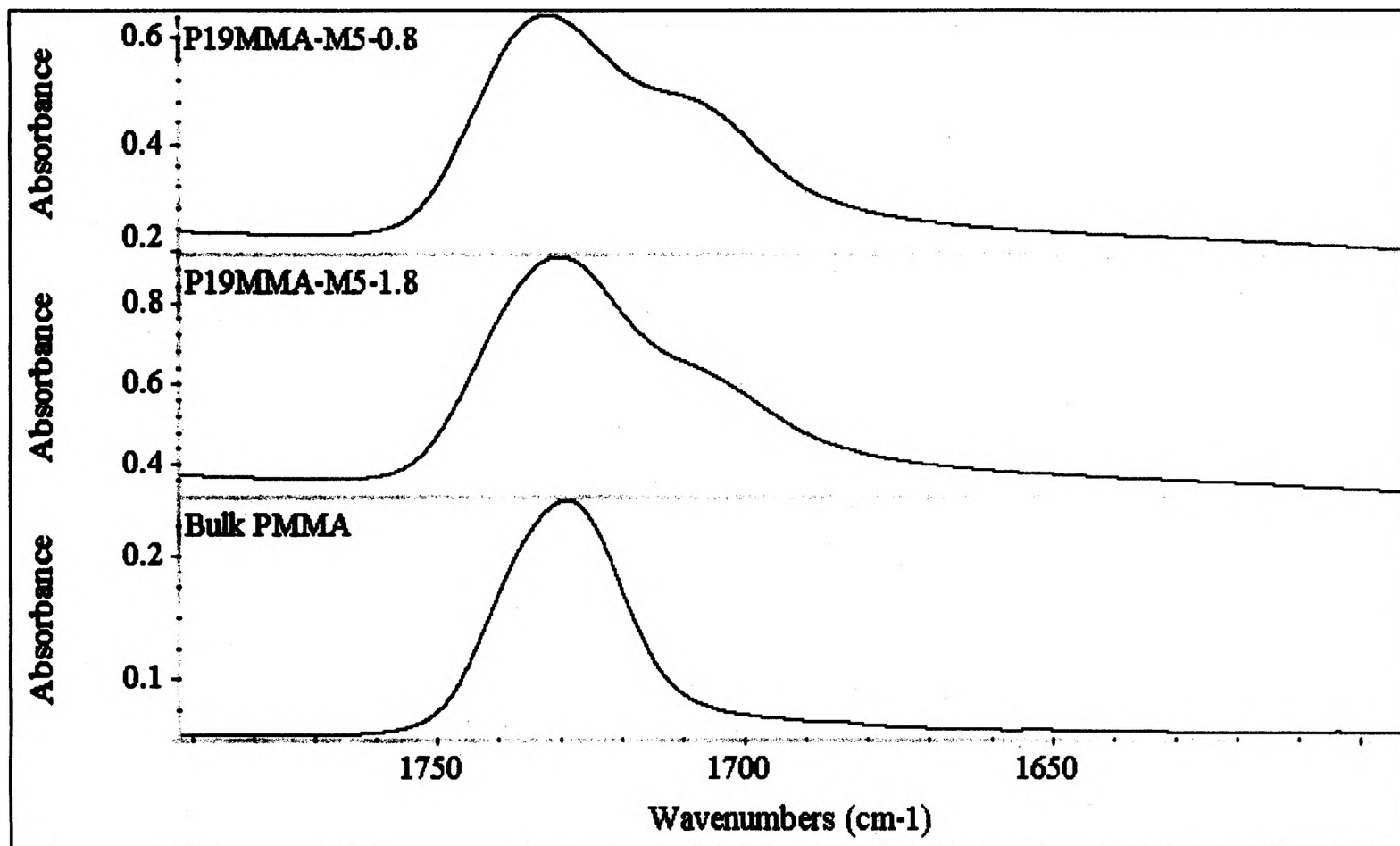


Figure 3.5. FTIR spectra of bulk PMMA and P19MMA adsorbed on M5 in the region of the carbonyl absorption.



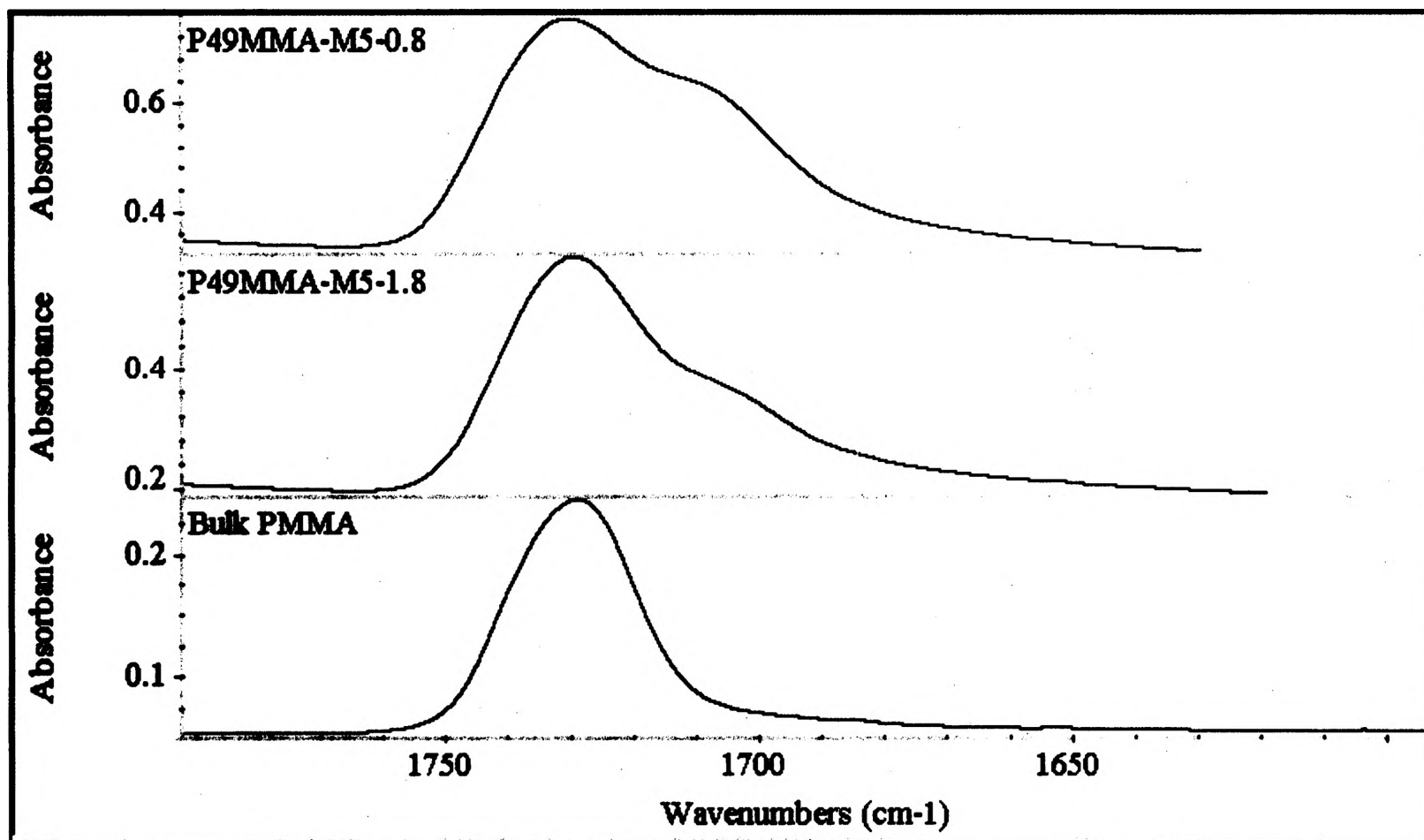


Figure 3.6. FTIR spectra of bulk PMMA and P49MMA adsorbed on M5 in the region of the carbonyl absorption.

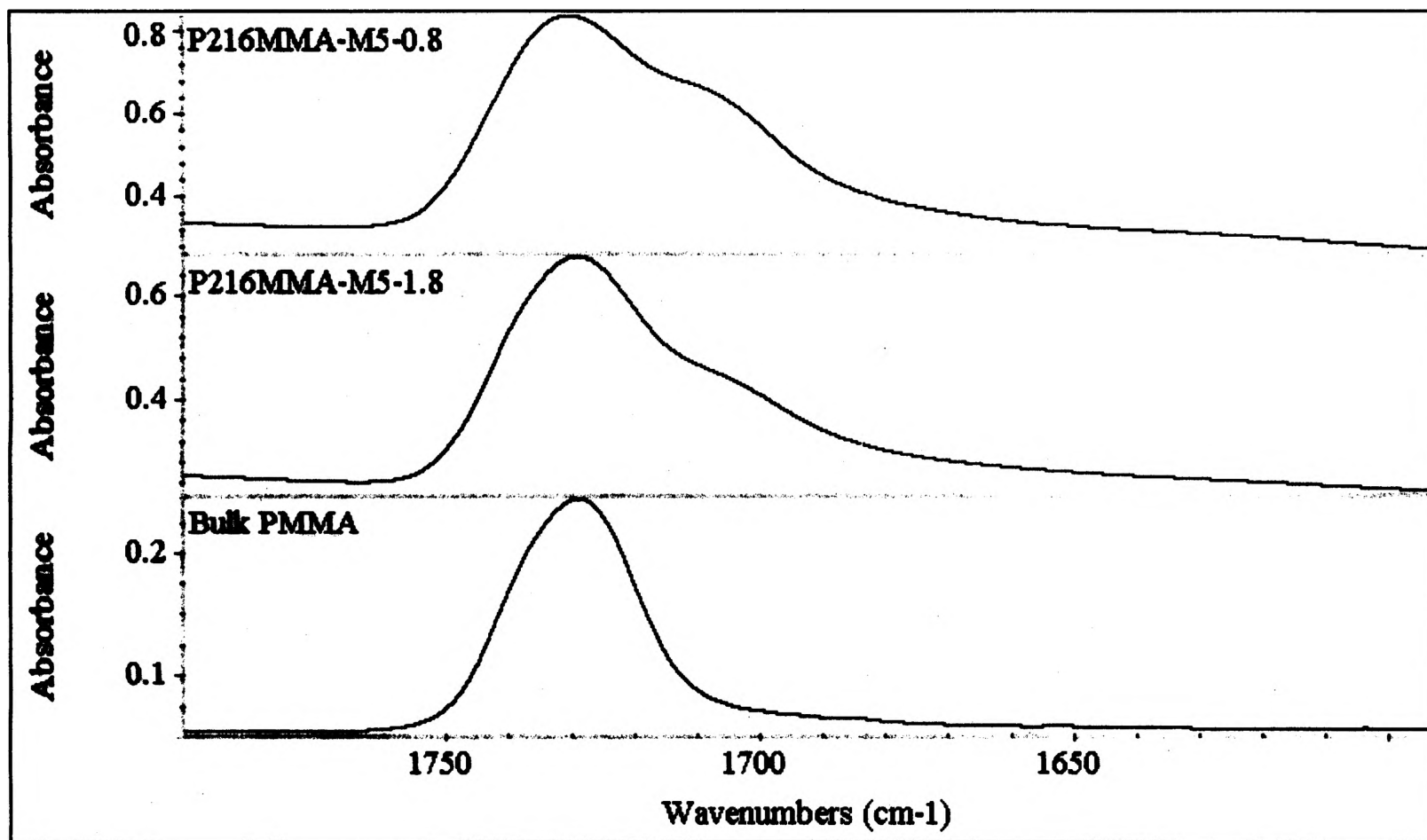


Figure 3.7. FTIR spectra of bulk PMMA and P216MMA adsorbed on M5 in the region of the carbonyl absorption.

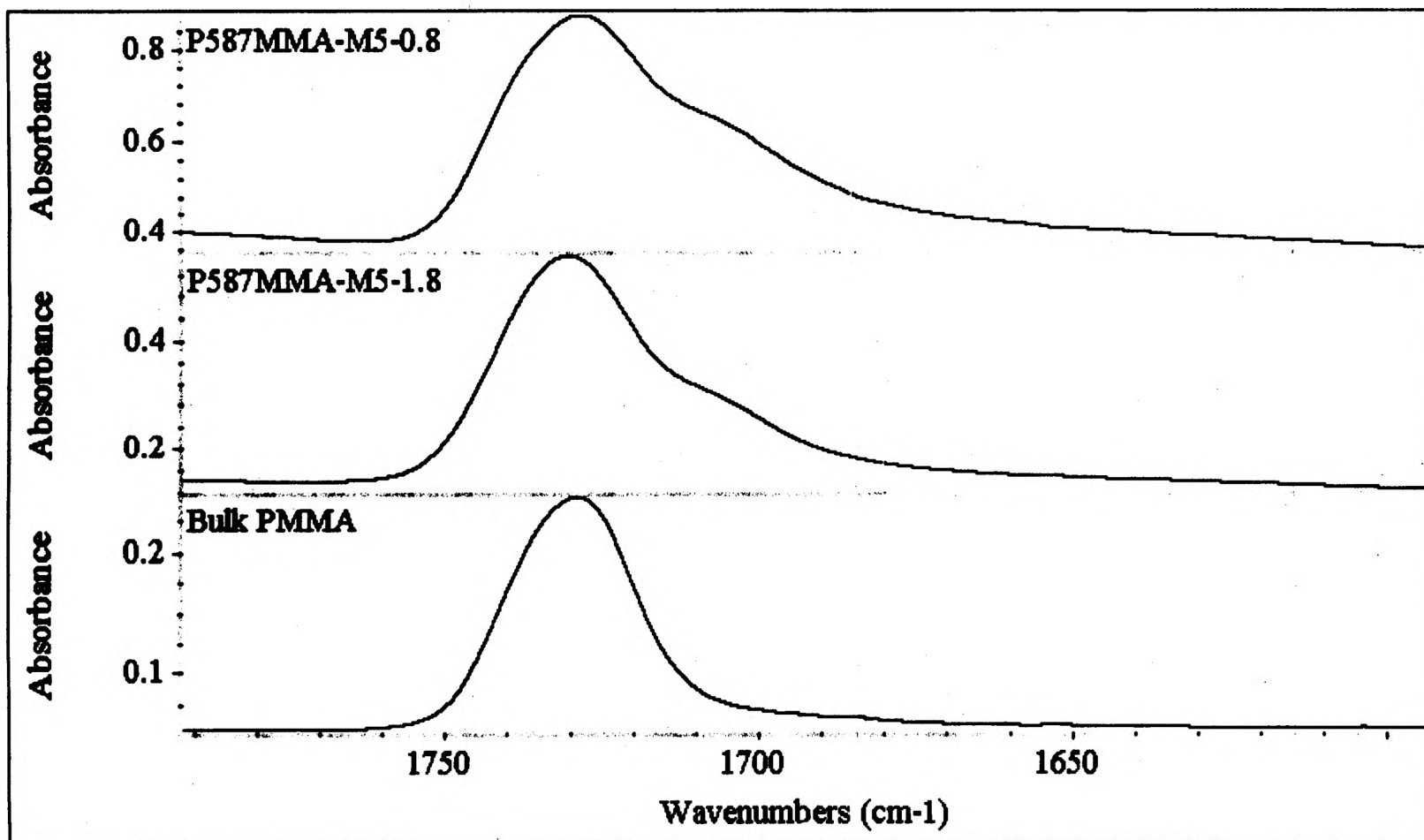


Figure 3.8. FTIR spectra of bulk PMMA and P587MMA adsorbed on M5 in the region of the carbonyl absorption.

Table 3.4. Bound Fractions for the PMMA Adsorbed Samples

Sample	Adsorbed Amount (mg/m <sup>2</sup> )	Bound Fraction	Bound Fraction/Adsorbed Amount
P19MMA-M5-0.8	0.84	0.46	0.55
P49MMA-M5-0.8	0.84	0.44	0.52
P216MMA-M5-0.8	0.81	0.45	0.55
P587MMA-M5-0.8	0.80	0.44	0.55
P19MMA-M5-1.8	1.4	0.34	0.24
P49MMA-M5-1.8	1.6	0.36	0.23
P216MMA-M5-1.8	1.7	0.36	0.21
P587MMA-M5-1.8	1.9	0.38	0.20

polymers. But it should be noted that the same values of bound fraction do not necessarily imply the same conformations. The same value of the bound fraction may be found for a chain with a few long trains and for one with many short trains.<sup>28</sup> At 10 mg/mL the expected variation of adsorbed amount with molecular weight was observed. The bound fractions decreased slightly with increasing molecular weight, shown by dividing the bound fraction with the corresponding adsorbed amount.

These results are in agreement, though not as pronounced, with those of Granick *et al.*<sup>29</sup> Using infrared spectroscopy in attenuated total reflection mode (FTIR-ATR) they observed a decrease in the bound fraction with increasing molecular weight of surface saturated PMMA samples adsorbed on oxidized silicon from carbon tetrachloride. But they also observed a molecular weight dependence of the chain conformation on surfaces with less than the maximum adsorbed amount which we did not observe.

It is worthwhile to point out that the glass transition of the adsorbed polymer seemed to be insensitive to molecular weight in contrast to their behavior in bulk. In bulk, the  $T_g$  increased with molecular weight, 116 °C and 133 °C for the lowest and highest molecular weight, respectively. The  $T_g$  of the adsorbed polymers were however similar, indicating a larger shift in  $T_g$  for P19MMA. The  $T_g$  of polymers decreases with decreasing molecular weight because of the extra free volume created by chain ends.<sup>30</sup> Theoretical models of polymer adsorption predict an increase in the fraction of tail segments,  $v_{ul}$ , and the number of tails per chain,  $n_{tl}$ , with molecular weight.<sup>25</sup> The number of tails per chain increases from zero for monomers to two tails per chain for very long polymer chains. This being so, we believe that the low molecular weight polymer suffers

a larger decrease in free volume, and a larger increase in  $T_g$ , upon adsorption because of the lower  $v_{fl}$  and  $n_{fl}$ .

The behavior of PMMA adsorbed on silica treated with HMDS was different from that of PMMA on untreated silica. The surface treatment of silica with HMDS replaces most of the surface hydroxyl groups with  $-\text{OSiMe}_3$  groups.<sup>31</sup> This renders the surface quite hydrophobic. Whereas the adsorption of PMMA from 10 mg/mL solutions on M5 afforded adsorbed amounts in the range 1.4-2.0 mg/m<sup>2</sup>, the adsorption of PMMA samples from these solutions on TS530 yielded only about 0.8 mg/m<sup>2</sup>. The MDSC curves of the PMMA samples on TS530 are shown in Figure 3.9. Figure 3.10 shows an infrared spectrum of PMMA on TS530. The transitions are slightly broadened but are centered around the bulk  $T_g$  (Table 3.5) indicating that a large fraction of the polymer segments exists at the polymer-air interface. When Fryer *et al.* studied the dependence of the  $T_g$  of polymer films on interfacial energy and thickness, they observed the  $T_g$  could be elevated or depressed relative to the bulk value depending on the strength of the interaction between the polymer segments and the surface.<sup>32</sup> The  $T_g$  of the polymer films decreased below the bulk value at low values of interfacial energies and increased at high values of interfacial energies. They attributed the decrease in  $T_g$  due to increased segmental mobility at low interfacial energies. Our results are not in contradiction but differ from those of Fryer *et al.* in that we did not observe any decrease in the glass transition for the PMMA films on the hydrophobic TS530.

### **3.5. CONCLUSION**

We have used modulated differential scanning calorimetry to study the glass transition behavior of PMMA thin films on silica. We have demonstrated that for strong polymer-substrate interactions the glass transition broadens towards high temperatures because of restricted and heterogeneous segmental mobilities. The intensity of the glass transition curves was more skewed towards high temperatures with decreasing adsorbed amount. FTIR spectroscopy revealed that this was because the bound fraction increased with decreasing adsorbed amount.

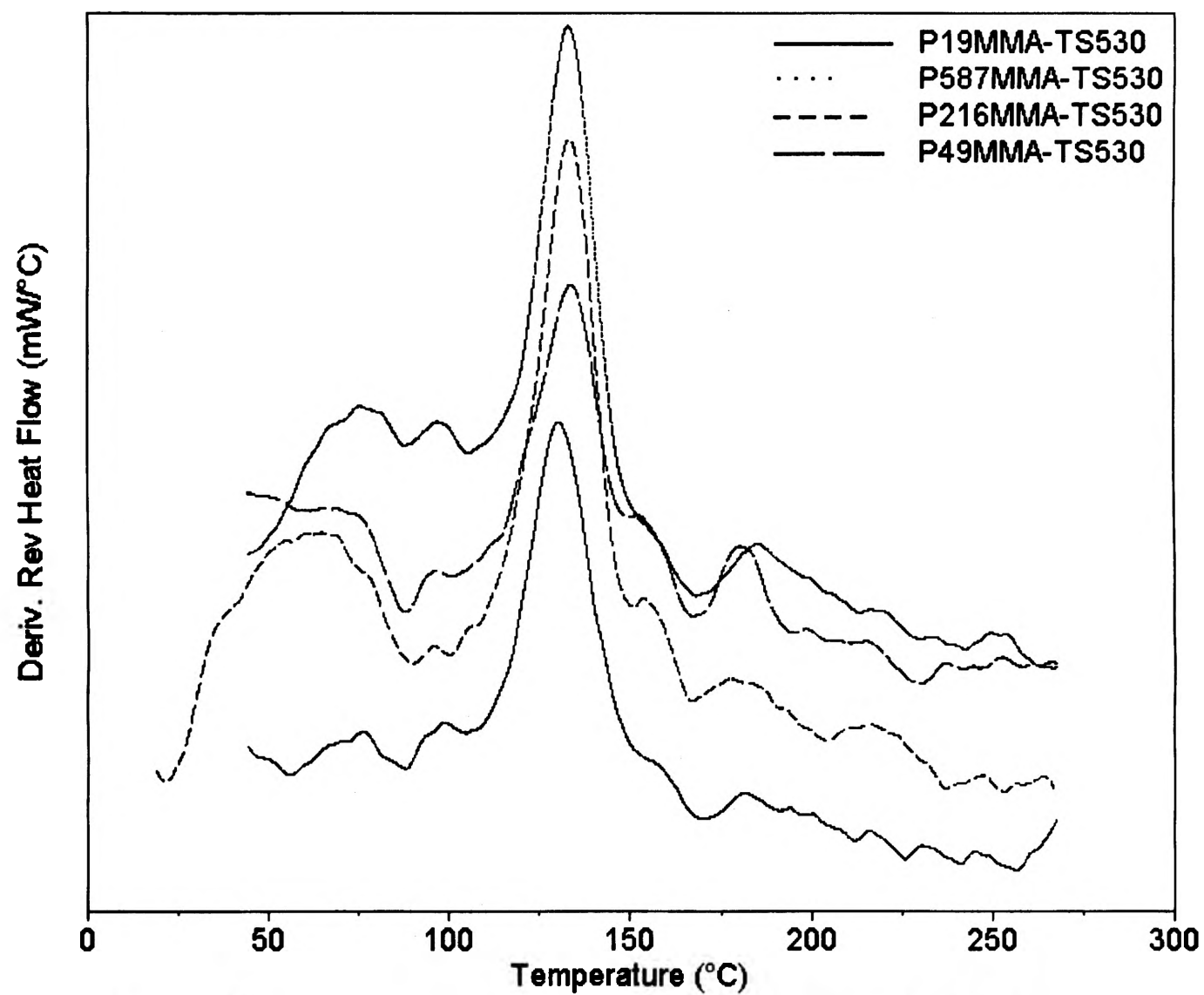


Figure 3.9. MDSC curves of PMMA adsorbed on TS530 from 10 mg/mL solutions.



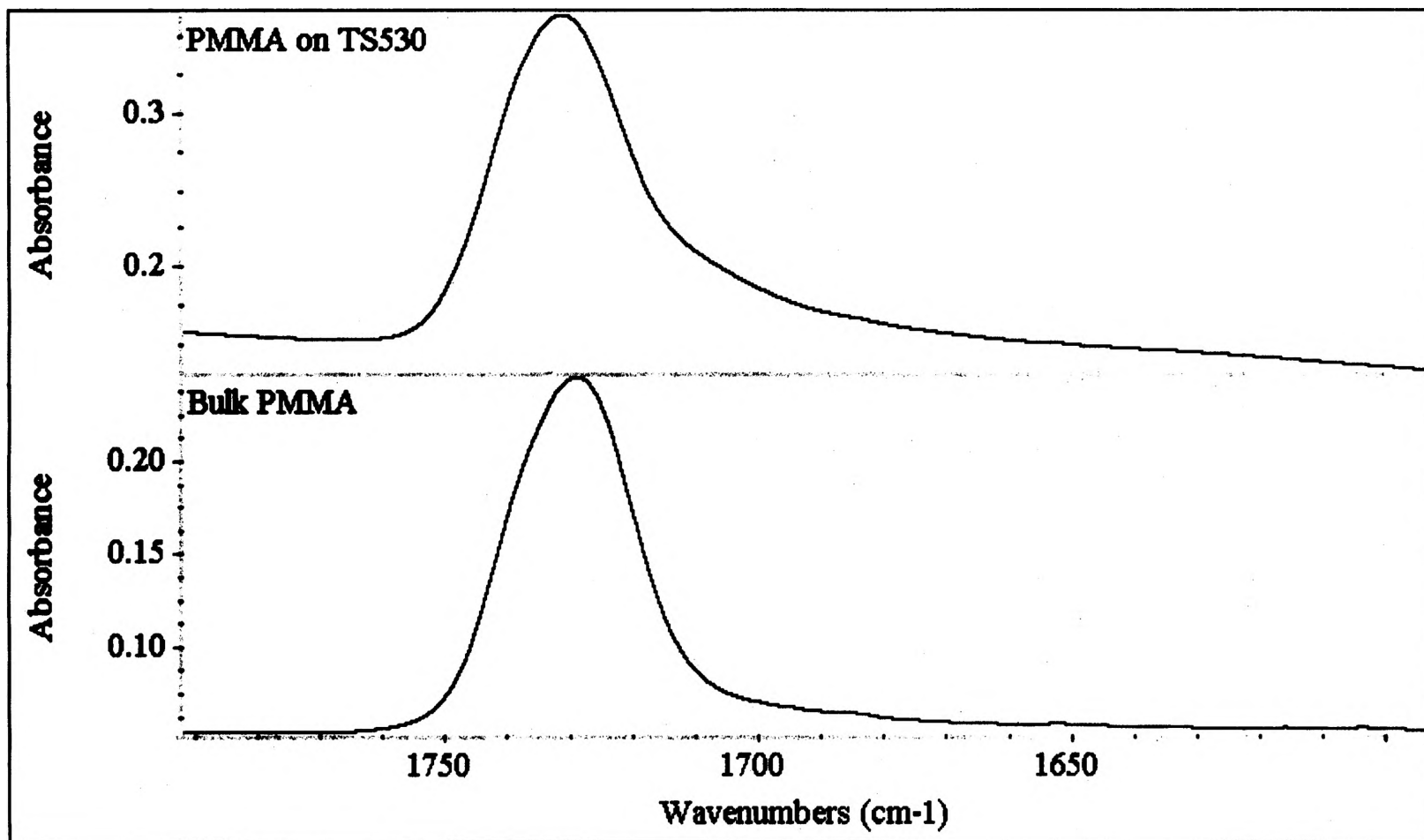


Figure 3.10. FTIR spectra of bulk PMMA and PMMA adsorbed on TS530 in the region of the carbonyl absorption.

Table 3.5. Thermal Characterization of the PMMA thin films adsorbed from 1% toluene solutions onto TS530 (treated silica).

Sample	T <sub>g</sub> (°C)	Transition Width (°C)
P19MMA	131	19
P49MMA	133	20
P216MMA	133	18
P587MMA	133	19

### 3.6. REFERENCE

1. Grohens, Y.; Brogly, M.; David, M.; Schultz, J. *Langmuir* **1998**, *14*, 2929.
2. Keddie, J. L.; Jones, R. A. L.; Cory, R. A. *Faraday Discuss.* **1994**, *98*, 219.
3. van Zanten, J. H.; Wallace, W. E.; Wu, W. *Phys. Rev. E* **1996**, *53*, R2053.
4. Wang, X. P.; Xiao, X.; Tsui, O. K. C. *Macromolecules* **2001**, *34*, 4180.
5. Kim, J. H.; Jang, J.; Zin, W. *Langmuir* **2001**, *17*, 2703.
6. Forrest, J. A.; Danolki-Veress, K.; Dutcher, J. R. *Phys. Rev. E* **1997**, *56*, 5705.
7. Kim, J. H.; Jang, J.; Zin, W. *Langmuir* **2000**, *16*, 4064.
8. Jones, R. A. L. *Current Opinion in Colloid and Interface Science* **1999**, *4*, 153.
9. DeMaggio, G. B.; Frieze, W. E.; Ming, Z.; Hristov, H. A.; Yee, A. F. *Phys. Rev. Lett.* **1997**, *78*, 1524.
10. Lin, W.; Blum, F. D. *Macromolecules* **1997**, *30*, 5331.
11. Mirau, P. A.; Heffner, S. A. *Macromolecules* **1999**, *32*, 4912.
12. Fukao, K.; Uno, S.; Miyamoto, Y.; Hoshino, A.; Miyaji, H. *Phys. Rev E* **2001**, *64*, 1.
13. Fukao, K.; Miyamoto, Y.; *Phys. Rev. E* **2000**, *61*, 1743.
14. Fryer, D. S.; Nealey, P. F.; de Pablo, J. J. *Macromolecules* **2000**, *33*, 6439.
15. Pollock, H. M.; Hammiche, A. J. *Phys. D: Appl. Phys.* **2001**, *34*, R23.
16. Pollock, H. M.; Hammiche, A.; Conroy, A.; Mills, G.; Weaver, M. R.; Price, D. M.; Reading, M.; Hourston, D. J.; Song, M. *J. Vac. Sci. Technol.* **2000**, *18*, 1322.
17. Pollock, H. M.; Hammiche, A.; Reading, M.; Hourston, D. J.; Song, M. *Polymer* **1995**, *36*, 3313.
18. Simon, S. L.; McKenna, G. B. *Proc. NATAS 29<sup>th</sup> Ann. Conf.* **1998**, 450.
19. Porter, C. E.; Blum F. D. *Macromolecules* **2000**, *33*, 7016.

20. Berquier, J.; Arribart, H. *Langmuir* **1998**, *14*, 3716.
21. Rosen, S. L. *Fundamental Principles of Polymeric Materials*; John Wiley and Sons: New York, 1993.
22. Keddie, J. L.; Jones, R. A. L.; Cory, R. A. *Europhys. Lett.* **1994**, *27*, 59.
23. Wallace, W. E.; van Zanten, J. H.; Wu, W. *Phys. Rev. E* **1995**, *52*, R3329.
24. Kawana, S.; Jones, R. A. L. *Phys. Rev. E* **2001**, *63*, 021501.
25. Fler, G. J.; Cohen Stuart, M. C.; Scheutjens, J. M.; Cosgrove, T.; Vincent, B. *Polymers at Interfaces*; Chapman and Hall: London, 1993.
26. Hourston, D. J.; Song, M.; Hammiche, A.; Pollock, H. M.; Reading, M. *Polymer* **1997**, *38*, 1.
27. Sakai, H.; Imamura, Y. *Bull. Chem. Soc. Jpn.* **1980**, *53*, 1749.
28. Cohen Stuart M. A.; Fler, G. J.; Bijsterbosch, G. H. *J. Colloid Interface Sci.* **1982**, *90*, 321.
29. Soga, I.; Granick, S. *Coll. Surf. A* **2000**, *179*, 113.
30. Bueche, F. *Physical Properties of Polymers*; Interscience Publishers: New York London, 1962.
31. Slavov, S. V.; Sanger, A. R.; Chuang, K. T. *J. Phys. Chem. B* **2000**, *104*, 983.
32. Fryer, D. S.; Peters, R. D.; Kim, E. J.; Tomaszewski, J. E.; de Pablo, J. J.; Nealey, P. F.; White, C. C.; Wu, W. *Macromolecules* **2001**, *34*, 5627.

**APPENDIX A**  
**DETERMINATION OF ADSORBED AMOUNT BY THERMOGRAVIMETRIC**  
**ANALYSIS**

The determination of adsorbed amount was performed using a Hi-Res™ TGA 2950 Thermogravimetric Analyzer (TA Instruments, New Castle, DE). Adsorbed PMMA samples weighing between 10-15 mg were heated in the furnace from ambient temperature to 600 °C at a heating rate of 10 °C/min. The polymer decomposed between 320 and 400 °C. The samples were purged with N<sub>2</sub> gas at a rate of 50 cm<sup>3</sup>/min. A TGA thermogram for P216MMA-1% is shown in Figure A1.

The adsorbed amount,  $\Gamma$ , was calculated using the following expression;

$$\Gamma = \frac{\Delta W}{R \times A} \quad (A1)$$

where  $\Delta W$  is the weight loss in mg,  $R$  is the weight of the residue in mg, and  $A$  is the surface area of silica in m<sup>2</sup>/g. These calculations were based on the assumption that the residue was made up almost entirely of silica.

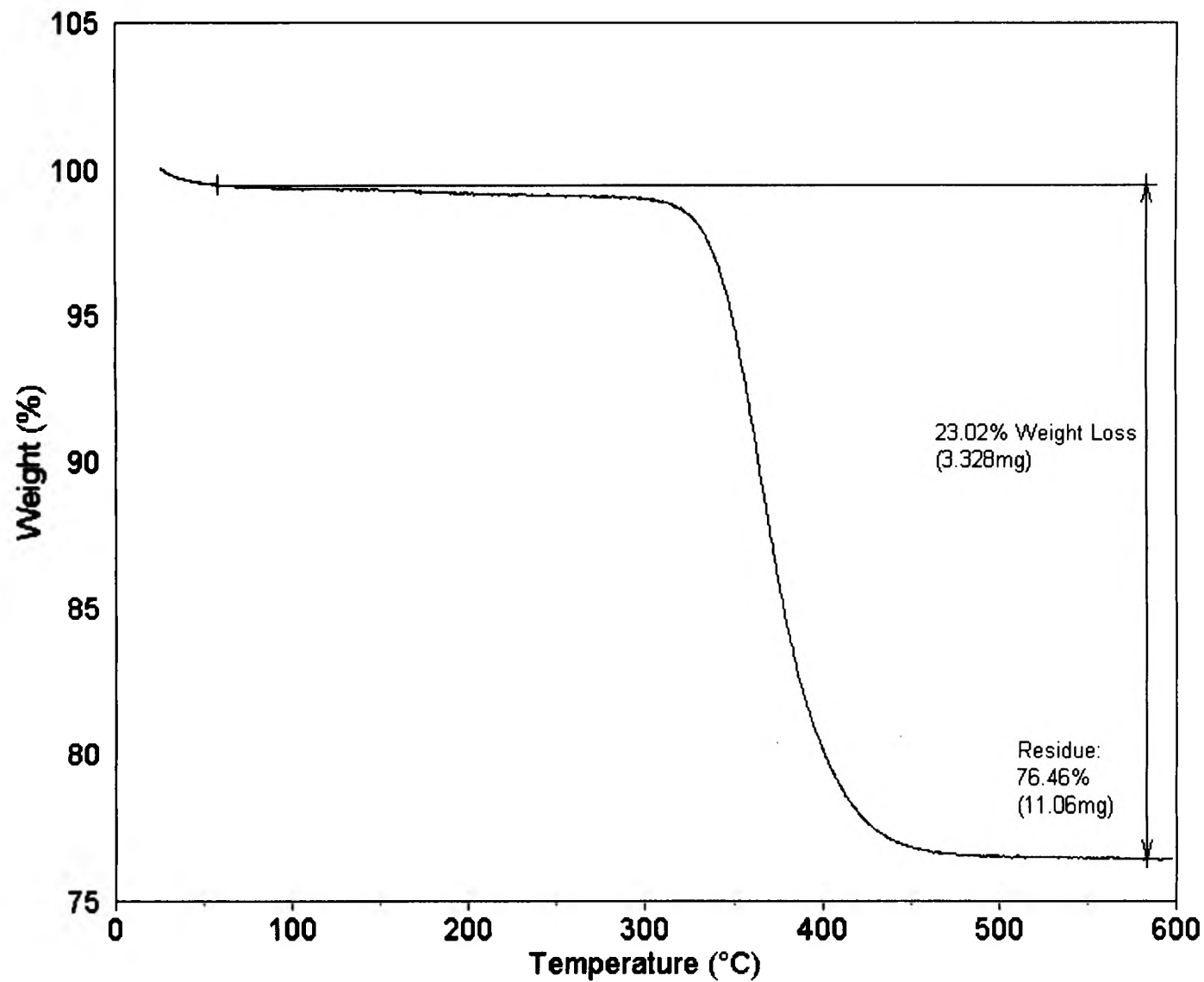


Figure A.1. Determination of the adsorbed amount by TGA. The sample was ramped from ambient temperature to 600 °C at a heating rate of 10 °C/min.

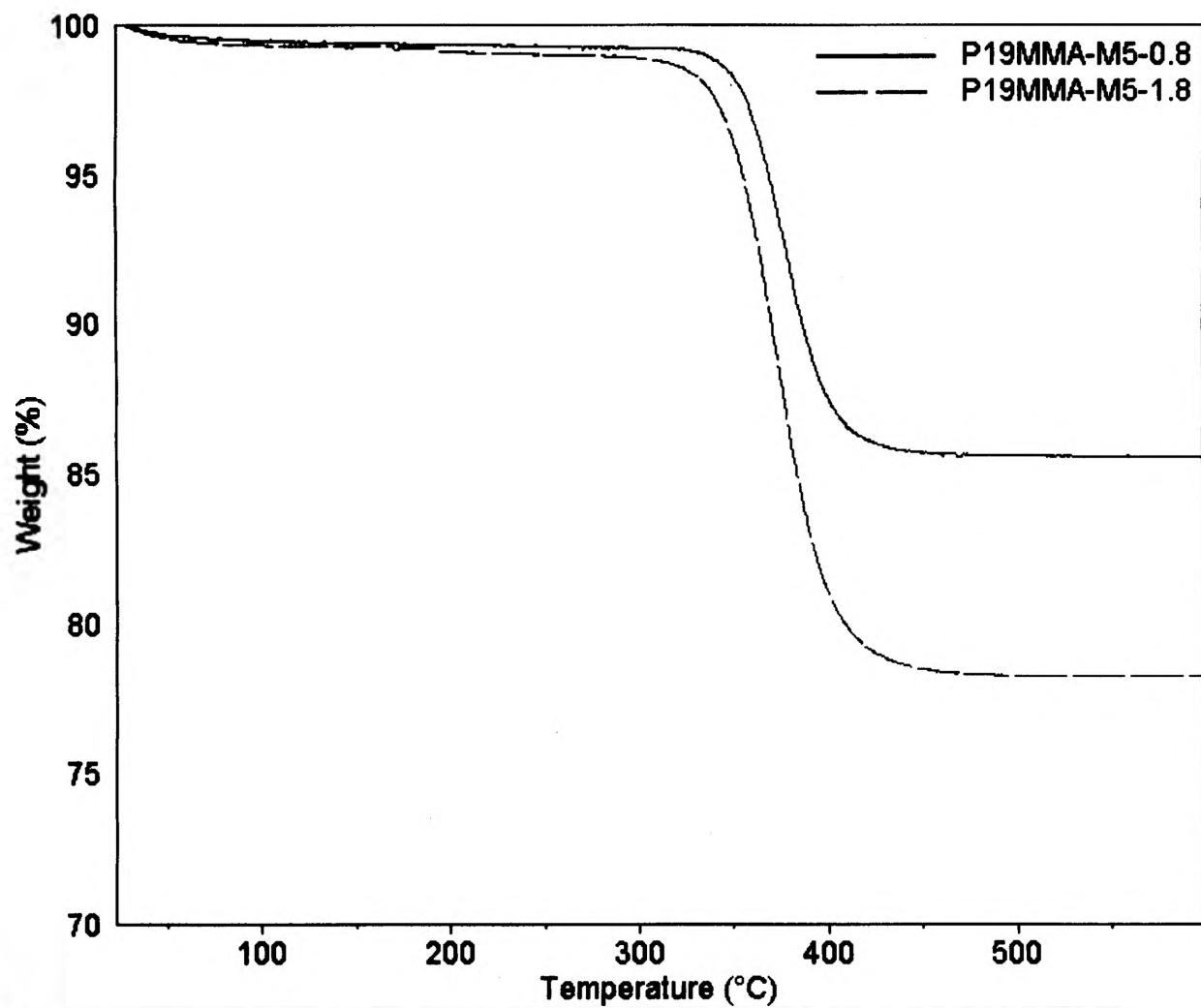


Figure A.2. TGA curves for the determination of adsorbed amount of P19MMA-0.8 and P19MMA-1.8. The samples were ramped from ambient temperature to 600 °C at 10 °C/min under nitrogen purge.



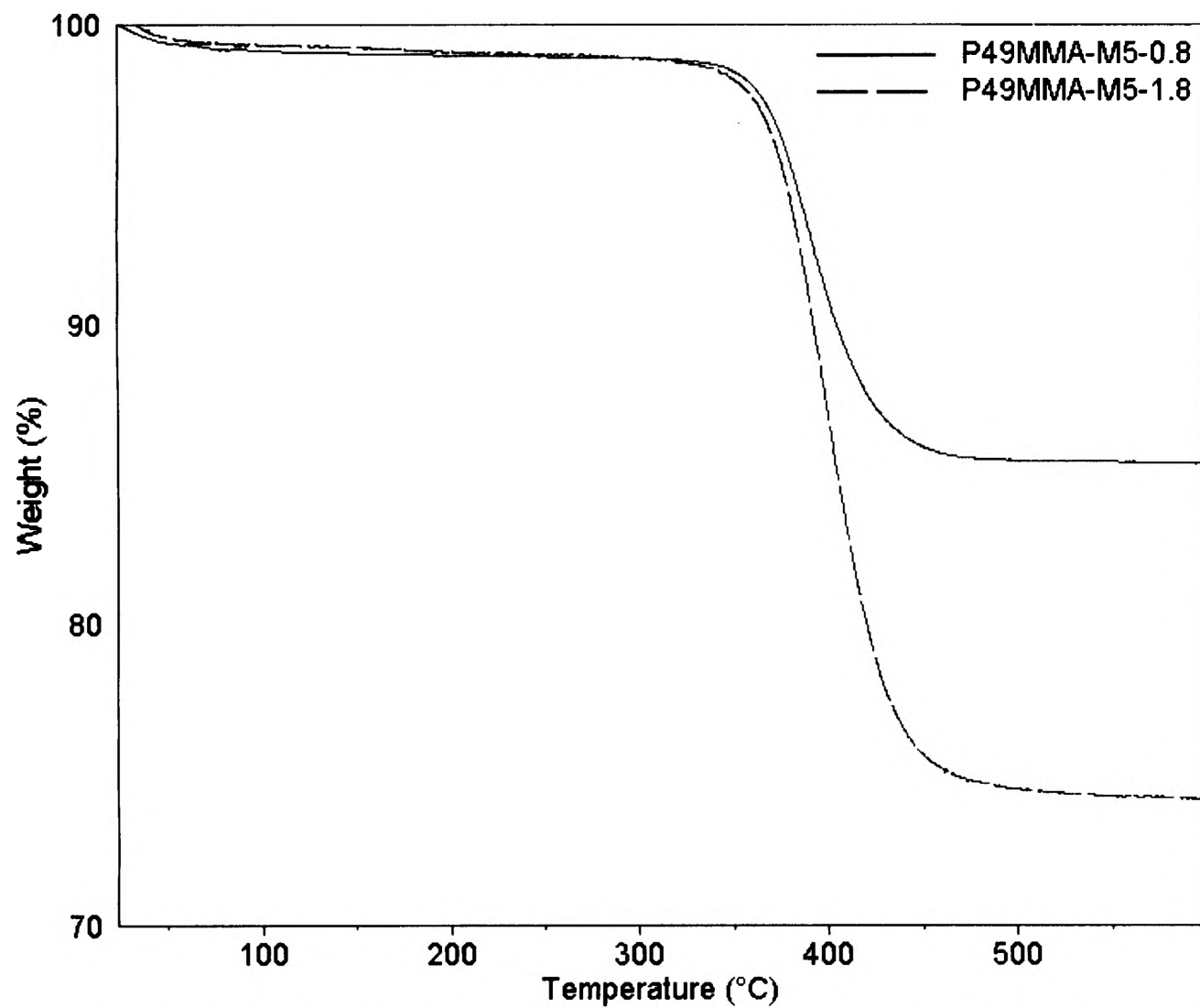


Figure A.3. TGA curves for the determination of adsorbed amount of P49MMA-0.8 and P49MMA-1.8. The samples were ramped from ambient temperature to 600 °C at 10 °C/min under nitrogen purge.

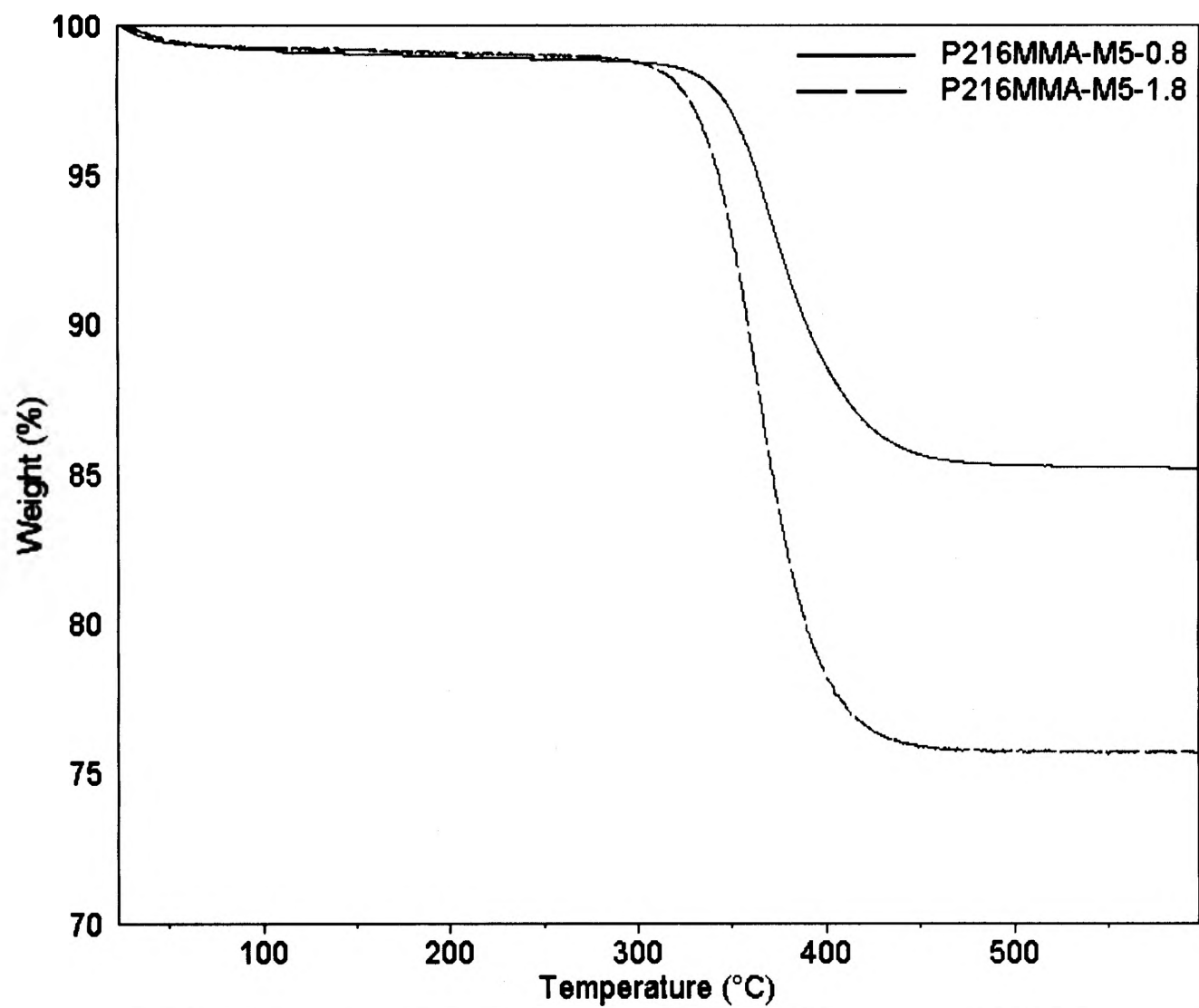


Figure A.4. TGA curves for the determination of adsorbed amount of P216MMA-0.8 and P216MMA-1.8. The samples were ramped from ambient temperature to 600 °C at 10 °C/min under nitrogen purge.

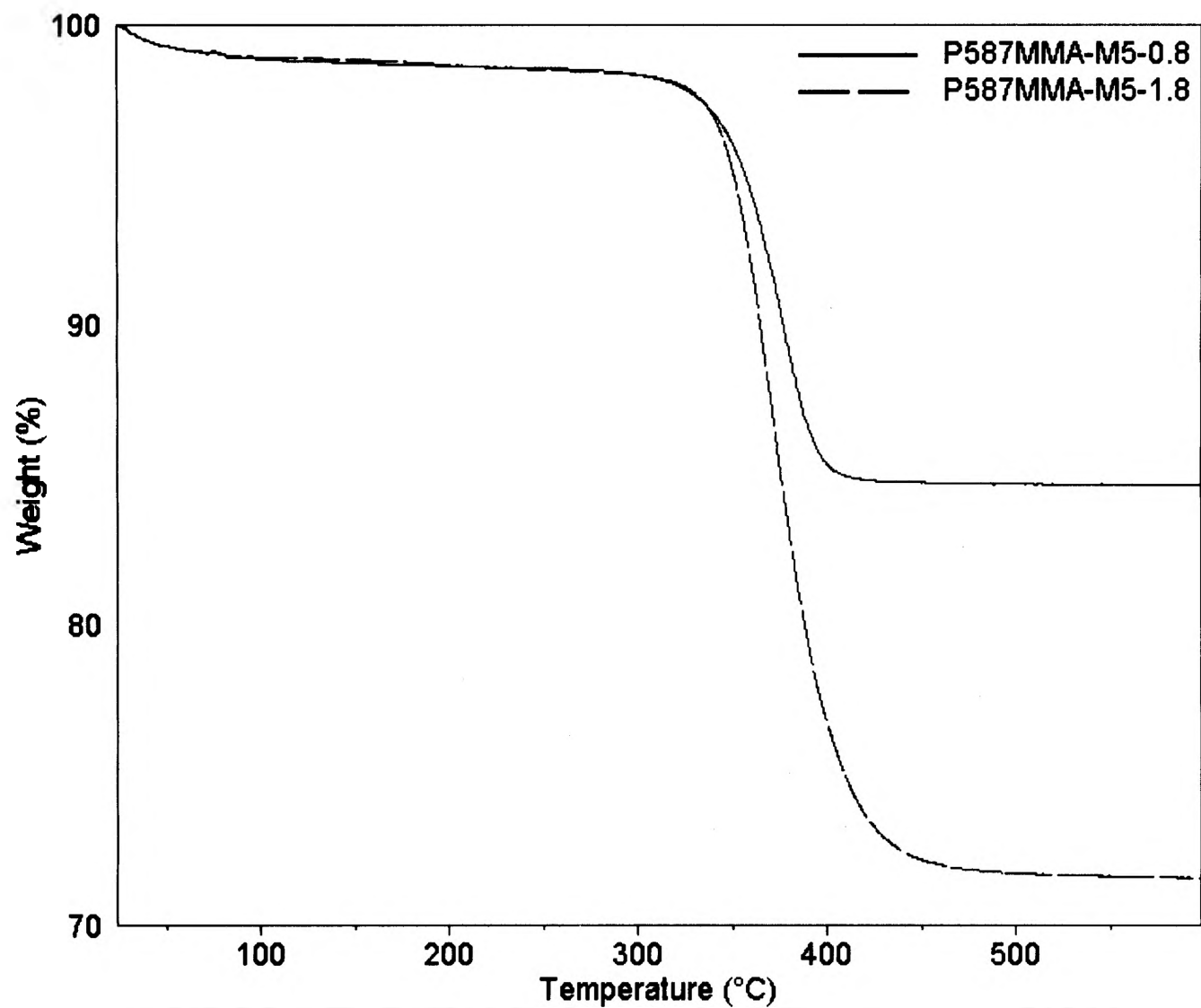


Figure A.5. TGA curves for the determination of adsorbed amount of P587MMA-0.8 and P587MMA-1.8. The samples were ramped from ambient temperature to 600 °C at 10 °C/min under nitrogen purge.

## **APPENDIX B**

### **INFRARED SPECTROSCOPY OF PMMA THIN FILMS ON SILICA**

Fourier transform infrared spectroscopy in the transmission mode was performed on thin films of bulk and silica-adsorbed PMMA prepared by solvent casting. Approximately 12 mg of sample were ground and a slurry was prepared by adding ca. 3 mL of toluene to the ground sample. A film of the slurry was cast on KBr cells. These were dried at room temperature for ca. 30 min and under vacuum at 70 °C for 1 hr.

FTIR spectra of the films were acquired for the range 4000 – 400  $\text{cm}^{-1}$  using a Nicolet Magna-IR™ Spectrometer 750 (Nicolet Analytical). 1024 scans were obtained. Absorbance spectra of bulk PMMA and adsorbed PMMA for the range 4000 – 400  $\text{cm}^{-1}$  are shown in Figures B.1 and B.2 respectively. The bound fractions were determined by curve fitting analysis of the carbonyl band using a trial version of Grams/32 AI software. An example is shown in Figure B.3.

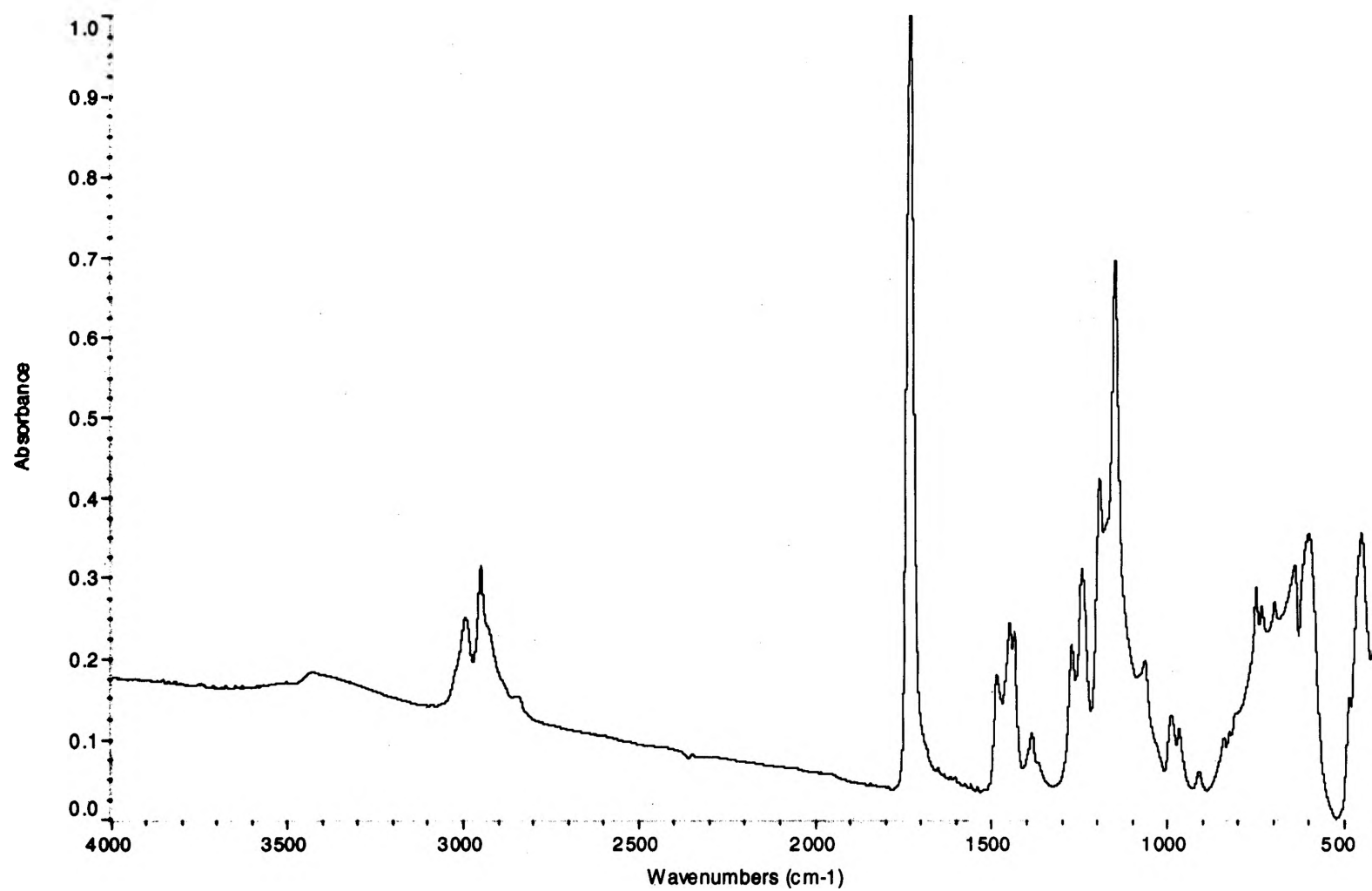


Figure B.1. FTIR spectrum of bulk PMMA acquired on a film cast from toluene. 1024 scans were performed to get good signal-to-noise ratio.

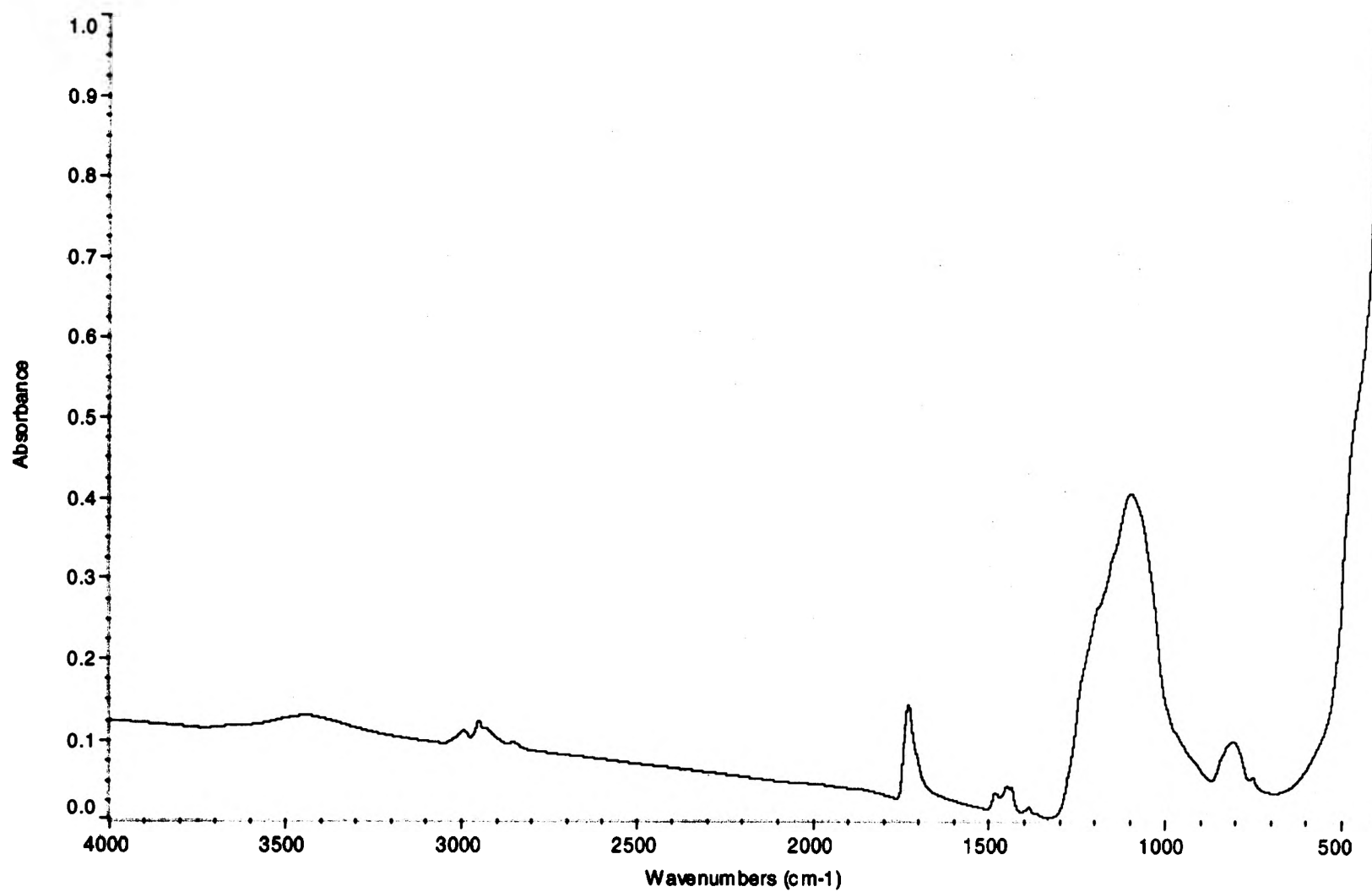


Figure B.2. FTIR spectrum of silica-adsorbed PMMA acquired on a film cast from toluene. 1024 scans were performed to get good signal-to-noise ratio.

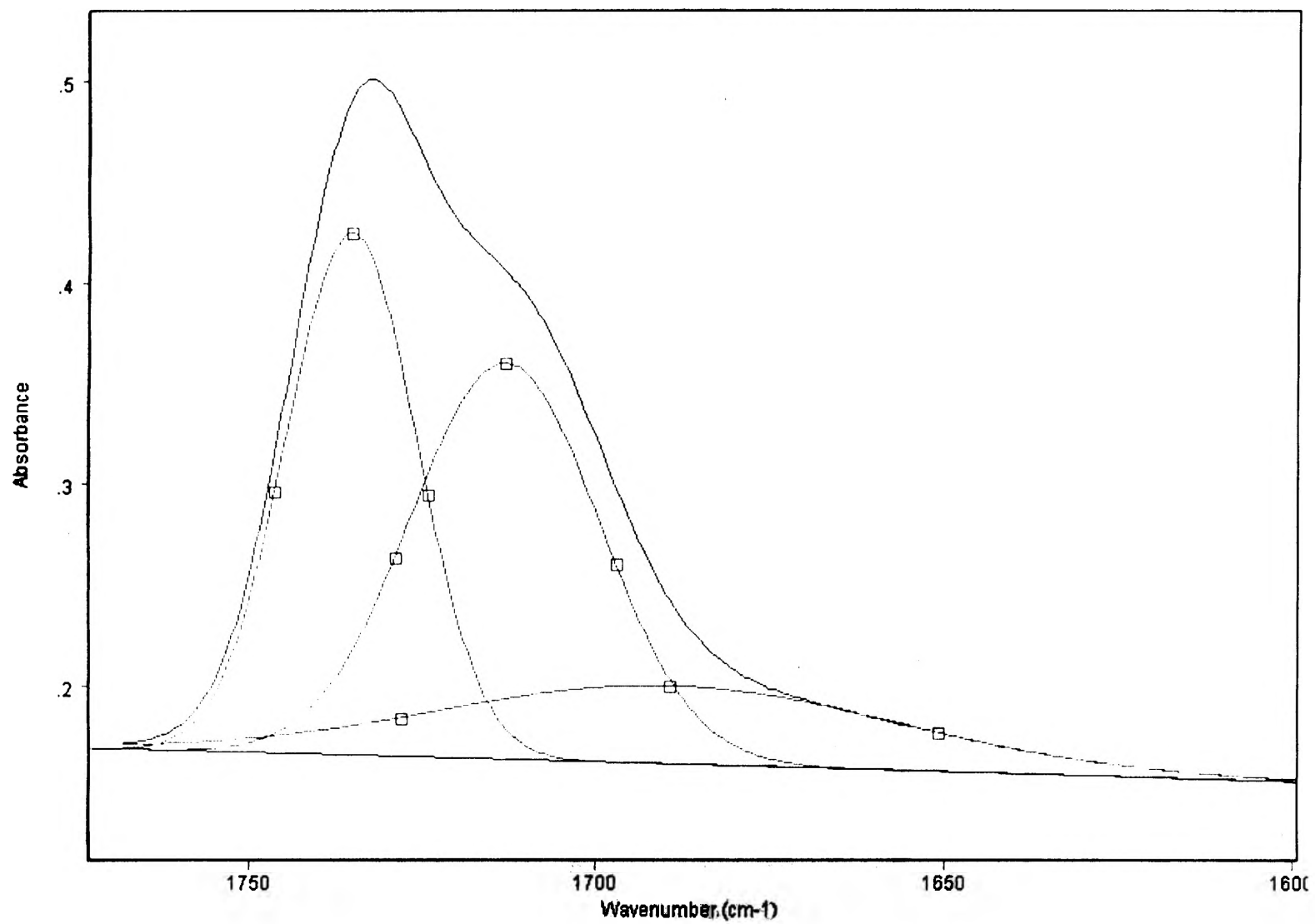


Figure B.3. FTIR curve-fitted carbonyl band of PMMA adsorbed on untreated silica (M5) from 0.5% toluene solution.



### VITA

Moses Tlhabologo Kabomo was born on July 3, 1974 in Gaborone, Botswana. He grew in up in the small diamond mining town of Jwaneng where he did his primary school and junior secondary school before going to boarding school to complete his O Levels. In January 1994, after one year of national service, Moses entered the Pre-Entry Science Course of the University of Botswana. He started his Bachelor of Science degree program in August 1994 and graduated in May 1998 with a Bachelor of Science Degree in Chemistry.

Before proceeding to the University of Missouri-Rolla for graduate studies, he worked for Plascon Paints in Gaborone and later joined the University of Botswana as a Staff Development Fellow in the Chemistry department. Moses Tlhabologo Kabomo entered the Chemistry program at the University of Missouri-Rolla in the year 2000 as a graduate student working for Dr Frank D. Blum.

Since he graduated from the University of Botswana, Moses has been an active member of the Rotaract Club of Gaborone for which he served as the Club President in 1999.